# Device-Context Based Indoor Localization

Chawin Terawong
Shanatip Choosaksakunwiboon
Suppakorn Suttisirikul


Bachelor of Engineering in Software Engineering
International College
King Mongkut's Institute of Technology Ladkrabang
Academic Year 2017
KMITL-2018-IC-B-003-010

**Thesis — Academic Year 2017**

Bachelor of Engineering in Software Engineering

International College

King Mongkut's Institute of Technology Ladkrabang

**Title:** : Device-context based Indoor Localization

**Authors:**


1. Ms. Chawin Terawong Student ID 57090004
2. Mr. Shanatip Choosaksakunwiboon Student ID 57090032
3. Mr. Suppakorn Suttisirikul Student ID 57090034


Approved for submission

(Dr. Isara Anantavrasilp)

Project Adviser

Date 8 / 6 / 2018

# Abstract

**Keywords: localization, indoor positioning system, RSSI, BLE, log-distance path loss model, channel separation**

Indoor localization has long been an active area of research, in order to overcome the problems of locating people or objects in an indoor environment. In this thesis, we propose a preprocessing technique that aims to improve the accuracy of indoor localization in healthcare application using Bluetooth Low Energy (BLE). This thesis analyzes the effect of BLE communication channels and device orientation on the accuracy of localization. The proposed channel separation preprocessing technique can improve distance estimation based on the Received Signal Strength Indicator (RSSI) of the Bluetooth signal by achieving a Root Mean Squared Error of 1.194 and standard deviation of 0.713, and achieving an RMSE as low as 0.154 for trilateration.

# Acknowledgements

We would like to express our deep gratitude to our advisor Dr. Isara Anantavrasilp and our co-advisor Asst.Prof.Dr. Surapa Thiemjarus for their advices and support on our project. The experience and knowledge we gained from our advisors were greatly valuable and our thesis would not be successful without their advices.

This work is supported in part by National Electronics and Computer Technology Center Thailand (NECTEC). The equipments and technologies used in our experiments, including BLE beacons and receivers, are provided by NECTEC.

We would also like to thank Asst.Prof.Dr. Chaiwat Nuthong, Dr. Ukrit Watchareeruetai, Asst.Prof.Dr. Visit Hirankitti and Dr. Natthapong Jungteerapanich for providing helpful comments and suggestions.

Finally, we would like to thank our colleagues for all the help and support on our project.

# Contents

# List of Figures

# List of Tables

# Chapter 1

# Introduction

## 1.1 Motivation

The application of satellite-based location services has long been widely accepted. Following the achievements of Global Positioning System (GPS), the focus has been shifted to Indoor Position System (IPS) which still remains a major challenge [13]. The indoor positioning services can provide guidance in complex facilities through mobile devices. Effective IPS would also enable the tracking of a person or an object.

In fact, several positioning methods can theoretically be used both indoors and outdoors. However, the system performances vary greatly according to the environmental factors. Indoor positioning are usually more difficult to achieve than outdoors due to several reasons such as signal scattering caused by the reflection from physical obstructions and the noise interference from signals from other devices nearby [22]. The outdoor positioning technology called Global Navigation Satellite Systems (GNSS) that is used in GPS provides accurate global localization with an error of less than 0.715 meters [20]. Unfortunately, satellite signal of GNSS performs poorly within buildings because the satellite signal cannot transmit easily through solid objects [22]. Before the satellite signal reaches the receiver in the building, its strength keep decreasing along the way as it travels through the air, roofs, walls and other obstacles.

In the end, the received signal strength will be too weak to be used for locating an indoor object.

Thus, researches on Indoor Positioning Systems become very popular in recent years. Still, not many satisfactory technical solutions have been proposed for indoor positioning applications. Some methods presented in the researches are fingerprint, triangulation and trilateration.

Our thesis proposes an improved device-context based indoor localization method that can locate people and moving objects in buildings by measuring the Received Signal Strength Indicator (RSSI) transmitted from the Bluetooth Low Energy (BLE) devices. BLE is one of the most commonly used technologies in mobile devices due to it's low power consumption and small sizes. This would allow our technique to be used in wide range of devices from smartphones to small tracking devices.

However, implementing localization on BLE is not a trivial task. Current BLE-based indoor positioning systems tend to suffer from low accuracy detection due to their ultra-low power consumption [28]. We believe, nonetheless, that localization accuracy can be improved by signal preprocessing.

## 1.2 Problem Statement

Performance of indoor positioning system using Bluetooth Low Energy can be improved by employing a signal preprocessing method.

## 1.3 Objective

The aims of the thesis are to explore different preprocessing techniques that can improve indoor localization accuracy based on device context information and showcase the visualization of the results real-time on the map in mobile devices. This thesis involves research to find the optimal approach for indoor localization and provide feasibility for deployment. The localization process

will be demonstrated through a mobile application displaying the location of a selected target object on a 2D map of a specific floor.

## 1.4 Scope of Work

The scope of our project only applies to an unobstructed environment and the preprocessing methods we propose are for BLE-based indoor localization. Our system provides a 2-D position of the target object and operates only in a single floor.

## 1.5 Thesis Structure

The rest of the thesis is organized as follows:

- Chapter 2 provides the background knowledge about indoor localization and related works.
- Chapter 3 describes the processes of the system and the methods that are used in each process.
- Chapter 4 describes different experiments done including data analysis and classification.
- Chapter 5 provides the evaluation of results and conclusion of the thesis.

# Chapter 2

# Background Knowledge and Related Works

Before describing our positioning approach , it is important to first understand the different properties of indoor positioning system and learn several existing solutions to indoor localization problems. This chapter present about indoor positioning system topologies, indoor localization methods, indoor positioning technologies and existing researches on various indoor positioning systems.

## 2.1 Topology of Positioning System

The Indoor Positioning Systems could be classified into four categories which are self positioning, remote positioning, indirect self positioning and indirect remote positioning systems. [11]

### 2.1.1 Remote Positioning

The first topology is called remote positioning. In this topology, mobile device (transmitter) will transmit the signal and many fixed measuring units (receivers) will receive the transmitted signal from the transmitter. After receiving the signal, the data of every fixed measuring unit will be transferred to the

master station. The master station will compute the location of mobile device according to the collected data. The overview of remote positioning system is depicted in Fig. 2-1.

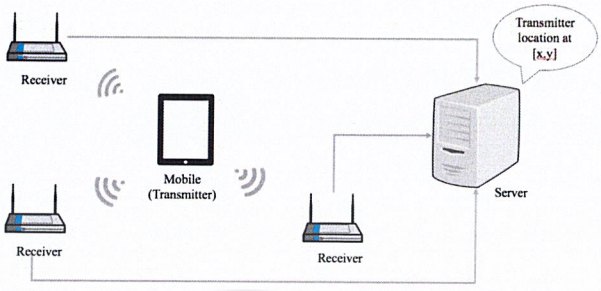


Figure 2-1: Remote Positioning.

### 2.1.2 Self Positioning

The measuring unit is the mobile device itself. The mobile device will receive the signals from many transmitters. All transmitters location must be fixed and the mobile device must know the location of every transmitter. After receiving the signal, the mobile device will calculate its position according to the location of the transmitters. The overview of self positioning system is shown in Fig. 2-2.

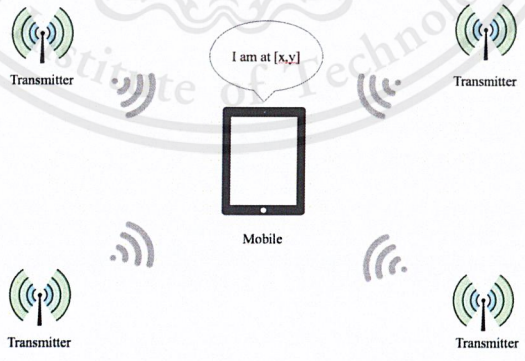


Figure 2-2: Self Positioning.

### 2.1.3 Indirect Self Positioning

In an indirect remote positioning, Signals will be collected at the fixed measuring units from the mobile device the same ways as in the remote positioning but in this topology the measurement result from the measuring unit will be sent to the mobile device. To sum up, it is a remote positioning system transmitting mobile device's position to the mobile device. Fig. 2-3 depicts the overview of indirect self positioning system.

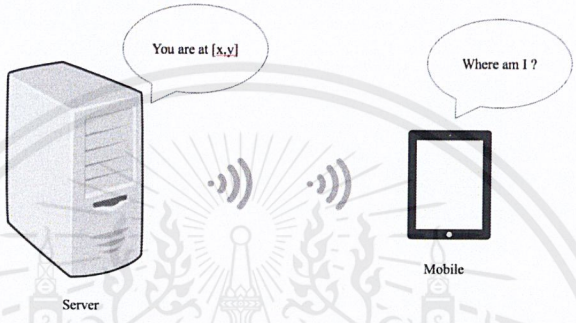


Figure 2-3: Indirect Self Positioning.

### 2.1.4 Indirect Remote Positioning

In this topology, mobile device will receive the signals from several transmitters in known locations as same as the self position topology. Then the mobile device will calculate the location and send to the remote location. In short, it is a self-positioning system that sends position data to a remote location. Fig. 2-4 depicts the overview of indirect remote positioning system.

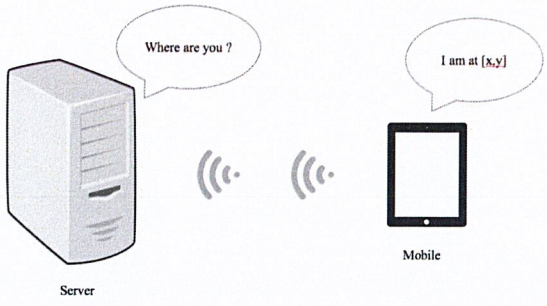


Figure 2-4: Indirect Remote Positioning.

## 2.2 Indoor Localization Methods

Various methods have been studied for indoor localization. In this section, three localization methods will be explained. The three methods are triangulation, trilateration and fingerprint-based method. All of the stated methods locate objects by measuring signals. The main type of signal used in indoor localization are infrared (IR) and radio frequency (RF) signal. This thesis will focus on using Bluetooth signal which is one type of RF signal.

### 2.2.1 Triangulation

Triangulation, or angle-based method, [5] is an estimation technique that uses trigonometric approach to determine a moving object's location. Two or more fixed reference nodes are required for location estimation by receiving mobile signals (e.g. Bluetooth signals) sent from the signal-transmitting device attached to the target object. The signals sent from the target node form a geometric relationship as shown in Fig. 2-5, which can further be used to estimate the location of the target object.

A technique used in triangulation is called the Angle of Arrival (AoA) technique. AoA-based technique determines the angle of arrival of the mobile signal sent from the target object at which it is received by multiple receivers. In

Fig. 2-5, the location of the target node $T_1$ is determined by measuring the angles of incidence ($\theta_1$, $\theta_2$) at which signals are sent from $T_1$ and arrive at the receiving nodes $R_1$ and $R_2$. Geometric relationships can be used to calculate the coordinate (X,Y) of the target node. However, AoA-based technique has certain drawbacks. AoA requires additional directional antennas to measure the angle of arriving signal which increases the cost of implementation. Furthermore, the technique performs poorly in a highly-obstructed environment. Signal reflections from walls and other obstacles cause signals to significantly change their direction and thus the angle of arrival [26].

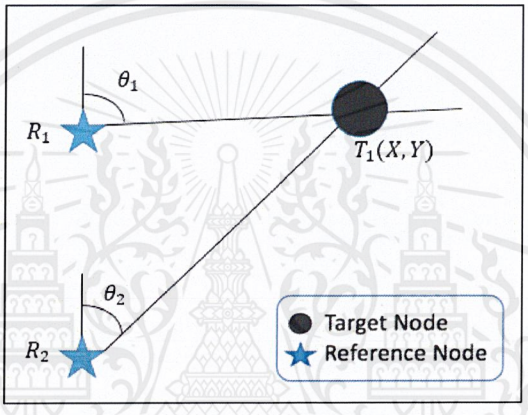


Figure 2-5: Angle of Arrival.

### 2.2.2 Trilateration

Trilateration, also called distance-based method, [5] is an estimation technique similar to triangulation, but requires at least 3 fixed reference nodes. The only difference between the two methods is that trilateration uses the distances between the receiving and transmitting nodes to calculate the coordinate of the target object, instead of the angles. In trilateration, the distances between the transmitter (target object) and receivers can be viewed as the radii of many circles with centers at the receivers. The intersection of all the circles is the location of the target object as seen in Fig. 2-6, where the coordinate of the target object ($X$,$Y$) can be estimated using the coordinates of the receivers (($X_1$,$Y_1$), ($X_2$,$Y_2$)

and ($X_3$,$Y_3$)) and the distances ($d_1$, $d_2$ and $d_3$). Trilateration can be subdivided into two categories namely time-based method and RSSI-based method [30].

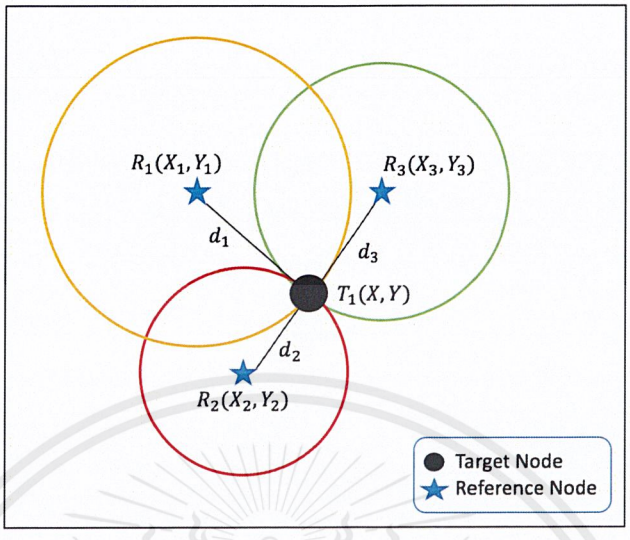


Figure 2-6: Trilateration.

**Time-Based Method**

In order to compute the distances between nodes, applying the time-based method is one of the option. As the name suggests, time-based method is based on the measurement of the signal propagation time. The 3 time-based techniques discussed in this section are Time of Arrival (ToA), Round Trip Time (RTT) and Time Difference of Arrival (TDoA).

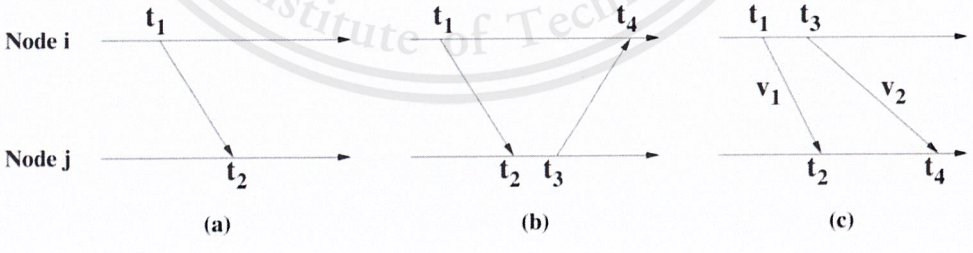


Figure 2-7: Trilateration using time-based methods

Time of Arrival (ToA) system calculates the distance based on the arrival time of a signal transmitted from the target object to the receivers. Fig. 2-7a

depicts a signal traveling at velocity v from the transmitting node i at time $t_1$ and reaching the receiving node j at time $t_2$. In ToA, the target object transmits a time-stamped signal, indicating the transmission start time, towards the receivers. Therefore, all receivers along with the target objects are synchronized with a precise time source. Once the signal is received, the distances between the transmitter (Node i) and the receivers (Node j) are calculated by measuring the transmission time delay and the corresponding signal speed as in Eq. (2.1) [27].

$$dist_{ij} = (t_2 - t_1) * v \tag{2.1}$$

Round Trip Time (RTT) finds out the distance by measuring the time that the signal takes to travel from the transmitter to the receiver and back. Fig. 2-7b shows the signal propagating back and forth between 2 nodes at different time. The distance equation is defined by Eq. (2.2) [27].

$$dist = \frac{(t_4 - t_1) - (t_3 - t_2)}{2} * v \tag{2.2}$$

In Time Difference of Arrival (TDoA), the relative time measured at each receivers is used instead of the absolute time. In this case, no clock synchronization is required. Fig. 2-7c shows 2 signals with different velocities v transmitted between 2 nodes. The first radio signal is sent at time $t_1$ and received at time $t_2$, then the following signal is sent at time $t_3$ and received at $t_4$, where $t_3$ = $t_1$ + $t_wait$ and $t_wait$ is the time gap between $t_2$ and $t_3$ when no signal is being propagated. The distance between the 2 nodes can be calculated by Eq. (2.3) [27].

$$dist = (v_1 - v_2) * (t_4 - t_2 - t_{wait}) \tag{2.3}$$

**RSSI-Based Method**

Another way to estimate the distance between the unknown node and the receiver is to measure the strength of the arriving signal called Received Signal Strength Indicator (RSSI) [30]. A transmitter attached to the target object emits

a radio signal to the reference node where the signal is received and its raw data is forwarded to the server. The server continues by extracting the RSSI feature from the signal for further computation of the distance. The RSSI measurement is heavily affected by the environmental interference, as the strength reduces significantly when the signal travels through obstacles. The model or the equation used to describe this propagation phenomenon and determine the distance between the transmitter and the receiver is known as the log-normal path loss model.

### 2.2.3 Fingerprint-Based Method

Fingerprint-Based method [25] is one of the popular techniques for indoor positioning due its high accuracy. The process of the fingerprint method consist of two main phases: training phase and classification phase. During the training phase we have to collect the RSSI data from each room of the target location and map the data into a classification model. After that, we train our system with the model we previously created. Next we go to the classification phase. In this phase the system will receive an input, which will be a RSSI sent from the target object, then it will classify the location of the target object via the model that it had learned. The fingerprint method can be a very accurate method with the use of a massive amount of data in the training phase. With that come a major disadvantage: it requires a lot of set up during the training phase. We need to collect large amount of data in order to just tell what room the device is in. To be able to track the device location with more precision the setup will be too impractical to be beneficial. And also the model that we use to train the system have to be proprietary to each location.

## 2.3 Indoor Localization Technology and System

Since GPS performs poorly in a building, different indoor positioning systems (IPSs) and technologies are studied in order to solve indoor positioning problems. Researches are carried out on different indoor localization methods and different technologies employed in indoor positioning systems. This section will describe several existing technologies used in the system to locate an indoor object. Gu and Lo's survey [29] divides IPSs into six categories according to the technologies employed.

### 2.3.1 Infrared Signals

Infrared (IR) light [3] is a light wave that is invisible to human eyes. IR is used by a remote control to change channels on TV. An IPS that uses IR light to locate an object is called an IR-based IPS. A disadvantage of IR-based IPS is that IR light cannot pass through opaque objects. Due to this limitation, the target object and the receiving sensor must be placed along the line-of-sight so that there are no obstacles in between. Thus, indoor localization with IR only works in a single room since IR light is blocked by walls. An example of IR-based IPS is the use of Active edge [14] worn by the target object that continuously transmits an IR signal providing an information about its location. A sensor detects the signal and uses the information from the signal to determine the location of the badge.

### 2.3.2 Radio Frequency

Radio Frequency (RF) is a measurement representing the oscillation rate of electromagnetic radio waves. It is one of the most important technology used in communication devices such as mobile phones and satellite TV to carry information. The main advantages of RF signal is that it can travel through solid obstacles so it does not require line-of-sight propagation. an IPS that uses RF

technologies is called RF-based IPS. Different forms of RF signal employed in RF-based IPS include Radio Frequency Identification (RFID), Ultra-wideband (UWB), Wireless Local Area Network (WLAN), WiFi, Bluetooth and Wireless Sensor Networks (WSN).

#### Radio Frequency Identification

Radio Frequency Identification (RFID) [24] systems consist of tags and reader devices. The tag gets activated by the RFID reader and returns a signal carrying the stored information. The process is analogous to the electronic barcode. The advantage of RFID technology is its robustness for the changes of lightness and noise. Using of RFID technology in indoor localization is common for tracking products in company or shopping malls and tracking patients in a hospital.

#### Ultra-wideband

Ultra-wideband (UWB) [8] is a short pulse, high frequency RF technology that spreads information out over a wide portion of frequency spectrum. Due to its high frequency, it is insensitive to interference of other radio signals and thus easy to filter. In wireless communication, the range of signal pulse greatly affects the accuracy. Since UWB emits a short pulse of signal, then the technology is better for short distance measurement. UWB can be used for indoor localization by utilizing the technique called Time Difference of Arrival (TDoA) on the UWB signal to compute the distance between the reference node (UWB receiver) and the target node (UWB transmitter).

#### Wireless Local Area Network and WiFi

Wireless Local Area Network (WLAN) [3] is a network in which a wireless router communicates with several WLAN compatible devices (e.g. laptop, mobile phone) through radio signals. Gu and Lo's survey [29] explains the implementation of WLAN IPS using radio frequency triangulation and fingerprint-

based technique. The survey shows that WLAN-based IPS has an accuracy error of several meters due to environmental influences and complex building facilities. WiFi is a type of WLAN and a widely adopted standards for communication. WiFi is a dominant wireless infrastructure that allows devices to communicate with one another wirelessly. Yang and Shao [4] presents a WiFi-based localization technique that improves the localization performance from the traditional trilateration technique. The article proposes a method that relaxes the need for wide signal bandwidth and the need for many receiving antennas by using the transmission of several predefined messages, and achieve 1 meter accuracy error.

**Bluetooth**

Bluetooth is wireless technology just like WiFi but operates in shorter range and lower data transfer rate. Its main advantages are battery-saving and low cost. BLE-based indoor localization using trilateration or range-based localization [6, 12] and fingerprint [23] are studied. These works suffer from low accuracy with an error up to 5 meters due to unstable RSSI caused by the ultra-low power consumption feature of the BLE device. Topaz location system [16] is an improved BLE-based IPS that has an error range of about two meters. Topaz integrates IR technology with the Bluetooth positioning and uses fingerprint-based method to obtain a higher robustness and accuracy.

**Wireless Sensor Networks**

A Wireless Sensor Network (WSN) is a wireless network consisting of several devices with sensors on them that perform collaborative measurement process. The sensors receive inputs from the external system and displays the received information. WSN-based IPS consists of 3 main components: sensor phase, protocol phase and application phase. Sensor phase is the collection of various sensors to receive data from the target environment. Protocol phase is any wireless

communication technology, such WiFi and bluetooth, that enables communication between sensors and application phases. Application phase consists of measurement and representation unit that provides interaction between user and system. Examples of application phase are any open source API, iOS and Android [3]. Cherntanomwong and Suroso [21] proposes WSN-based localization system employing trilateration and fingerprint technique. Both techniques result in error less than 1.2 meter.

### 2.3.3 Geomagnetic-field

Earth's geomagnetic-field can be used for indoor navigation. Human measures geomagnetic-field through compass to find directions. IndoorAtlas [2] presents indoor positioning system that involves magnetic field. The company provides an open source API for magnetic-field mapping. Magnetic-field mapping involves collecting the strength and direction of magnetic field at large number of locations, then mark each location with an arrow pointing in the measured direction of the magnetic field and its corresponding magnetic field strength, similar to fingerprint-based technique. An application named Easyshopping [17] utilize geomagnetic-field mapping in a shopping mall. The shopping carts contain a touch screen monitor that users can use to search for the location of a particular product and navigate the users to the shelf containing that product. The advantages of using geomagnetic-field technology are that it has no line-of-sight limitation meaning the geomagnetic field is able to operate in highly obstructed buildings and has large coverage area. The disadvantage is that the signal gets distorted in buildings due to steel girders or other metal materials, resulting in localization error.

### 2.3.4 Ultrasound Wave

Ultrasound wave is a type of inaudible sound wave that can travel through air and solid materials. The use of ultrasound wave can be seen in bats. Bats emit

ultrasound on an object and rely on the echo to navigate them in the darkness. Similar mechanism is used for indoor localization called the active bat system [10], equipped with matrix of fixed reference nodes that act as ultrasound receivers on the ceiling. The tag worn by a person will emit ultrasound signal then the signals are captured by the receivers on the ceiling. The location of the person is then calculated by applying the time-based trilateration method. Unlike infrared light wave, ultrasound wave does not require line-of-sight propagation, so it can locate hidden objects.

### 2.3.5 Audible Sound

Audible sound is a sound wave audible by human. It has properties that allow it to travel through air and solid objects. Audible sound wave can be emitted by every mobile devices such as mobile phones and laptops. Beep [9] studies IPS that utilize audible sound. Sound is typically sensitive to noise, so the localization process that uses audible sound will be degraded by noise interference. A possible solution is to operate audible sound-based IPS in a small, quiet environment.

### 2.3.6 Camera Positioning

The use of camera and computer vision technology for indoor localization is known as vision-based IPS. In [15], the micro-flyer equipped with two cameras take pictures of the special texture on the wall. By analyzing the distortion of the captured texture, the system can estimate its relative locations from the walls. The UAV (Unmanned Aerial Vehicle) in [19] shots laser beams to the surrounding. By capturing and analyzing the position of the laser points on the walls and ground, the UAV can predict its distance from ground and walls. However, vision based localization consumes significant amount of power and computing resources that are used to analyze the captured image. Furthermore, the use of camera will increase the cost of the system results in low scalability

of the system.

Table 2.1: Evaluation of Indoor Localization Technology.

| Technology | Advantage | Disadvantage |
|---|---|---|
| Infrared (IR) | - IR-based IPS is very accurate | - Line of sight limitation (IR-based IPS is limited in a single room)<br>- Can't travel through opaque objects<br>- Influenced by light source or sunlight<br>- Can't provide absolute location |
| Radio Frequency (RF): RFID | - Robust against environmental influences (e.g. light and noise)<br>- Can provide unique identification for each target object | - Implementation of the system is complex (requires many fixed reference nodes to provide good accuracy) |
| Radio Frequency (RF): UWB | - UWB-based IPS is accurate and precise<br>- Does not need line-of-sight transmission<br>- Can penetrate through solid obstacles | - Small coverage area (short signal range)<br>- UWB-based IPS is costly |
| Continued on next page | | |

Table 2.1: Evaluation of Indoor Localization Technology (continued).

| Technology | Advantage | Disadvantage |
|---|---|---|
| | - Robust against signal interference<br>- Can provide unique identification for each target object | |
| Radio Frequency (RF): WLAN | - WLAN-based IPS is easy to set up<br>- Readily deployed in building infrastructure | - WLAN-based IPS is not very accurate (error is several meters)<br>- Can be affected by other signals |
| Radio Frequency (RF): WiFi | - WiFi-based IPS is very accurate and fast<br>- Equipped in most compatible devices | -WiFi-based IPS is power-consuming |
| Radio Frequency (RF): Bluetooth | - Does not need line-of-sight transmission<br>- Equipped in most compatible devices | - Accuracy error up to 5 meters [6, 12, 23]<br>- Small coverage area (short signal range) |
| Radio Frequency (RF): WSN | - Does not need line-of-sight transmission | - WSN-based IPS is not very accurate (error is several meters) |
| Geomagnetic-field | - Does not need line-of-sight transmission<br>- Large coverage area | - Affected by metal obstacles |
| | | Continued on next page |

Table 2.1: Evaluation of Indoor Localization Technology (continued).

| Technology | Advantage | Disadvantage |
|---|---|---|
| Ultrasound Wave | - Does not need line-of-sight transmission<br>- Can penetrate through solid obstacles | - Affected by noise, thus cannot operate in large, crowded area |
| Audible Sound | - Does not need line-of-sight transmission<br>- Can penetrate through solid obstacles | - Affected by noise, thus cannot operate in large, crowded area<br>- Audible-sound based IPS creates noise while it is operating |
| Camera Positioning | - No multipath effect (signal reflection from obstacles has no effect)<br>- Use high level information to locate an object | - Line-of-sight limitation<br>- Power- and resource-consuming<br>- Costly (leads to low scalability of the system) |

Indoor positioning system still has many rooms for improvement (e.g. low accuracy, exhaustive deployment). In this thesis, we are focusing on improving distance estimation. To be precise, we will improve the distance estimation of BLE based indoor positioning system by applying data preprocessing on the RSSI of BLE to obtain an accurate distance estimation. Different methods of preprocessing such as channel separation, moving average and moving median are being explored in our research to achieve a better result of localization.

# Chapter 3

# Methodology

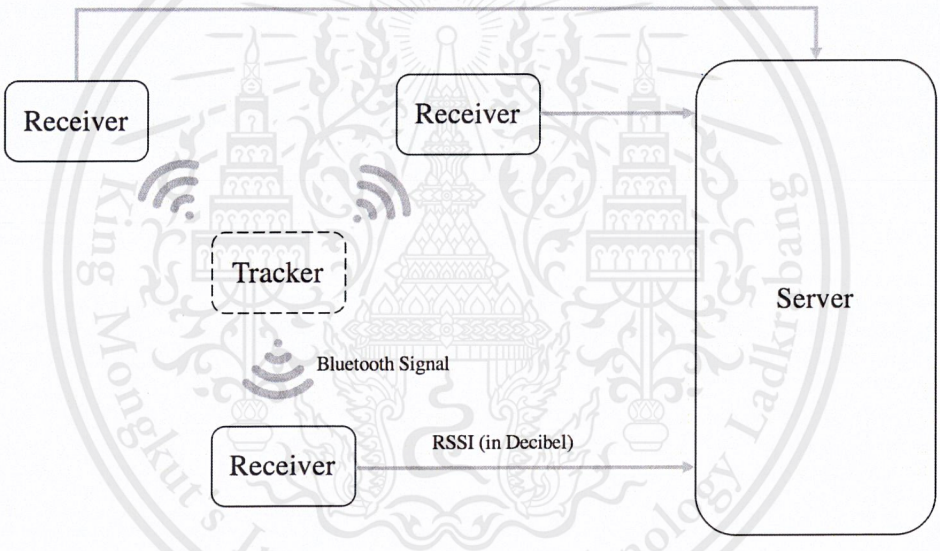


Figure 3-1: System topology.

In our research, we use the Remote Positioning topology as seen in Fig. 3-1. Receivers receive Bluetooth signals from the target tracker. The RSSI is being extracted from the signal then the RSSI is sent to the server. At the server, it preprocessed the RSSI data using moving average, moving median and channel separation. After preprocessed, server calculates the position of where the tracker location is in the target area using trilateration technique.

The tracker that we use is a BLE (Bluetooth Low Energy) device which transmits Bluetooth signal at the sampling rate of 10 Hertz. The receiver is used for receiving Bluetooth signal from the tracker in the form of RSSI (Received Signal Strength Indication) in decibel unit. Fig. 3-2 depicts the devices that we use to collect the RSSI data. Fig. 3-2a and Fig. 3-2c are the receivers used in our project, while Fig. 3-2b and Fig. 3-2d are the BLE trackers.

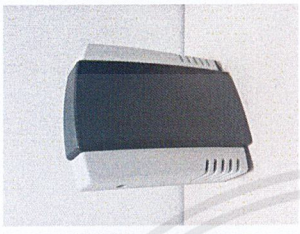

(a) BLE Anchor

(b) B4 Bracelet Beacon

(c) Raspberry Pi 3 Receiver

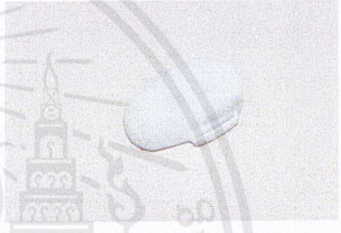

(d) AiR (Autonomous Intelligent Recognition) Node

Figure 3-2: Devices

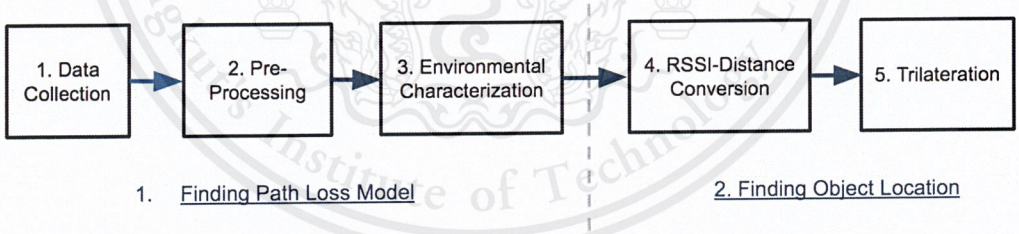


Figure 3-3: Overview of the System Processes.

The flow of methodology is as depicted in Fig. 3-3. The general processes of the system are divided into two main sections which are "Finding Path Loss Model" and "Finding Object Location." The "Finding Path Loss Model" section consists of three processes: Data Collection, Preprocessing and Environmental Characterization. The Data Collection process is the collection of a huge set

of RSSI data in a free-space environment at multiple known distances and different angle of rotation of the tracker as a training set by having the receivers receiving RSSI transmitted from the target object. In the Preprocessing process, the raw RSSI data is being preprocessed through several methods such as moving average, moving median and channel separation. In the Environmental Characterization process, a method called curve fitting is performed on the cleaned set of RSSI data to get the log-distance path loss model, in which the model is used to find the distance between the tracker and each receiver. Next in the "Finding Object Location" section, RSSI values are being measured continuously by the receivers. This section consists of two processes: RSSI-Distance Conversion and Trilateration. In the RSSI-Distance Conversion process, the measured RSSI values are preprocessed by the aforementioned methods and substituted into the corresponding log-distance path loss model to convert RSSI to distance. After this conversion, we are able to obtain the distances between the target object and the receivers. Finally in the Trilateration process, the trilateration equation is applied to determine the exact location of the target object. The overview of the system processes is depicted in Fig. 3-3.

This chapter will explain each process of our indoor localization methods in detail.

## 3.1 Finding Path Loss Model

### 3.1.1 Data Collection

The first process of this section is data collection. In our system, the tracker attached to the target object will transmit the Bluetooth signal at 2.4 GHz. The receivers then receive that signal from the tracker then extract the RSSI data from the incoming signal and send it to the server for further calculation.

Fig. 3-4 shows how the devices are set up in the data collection process. On the collection of data, the receiver and the tracker are placed on stands with a

height of 1.15m. The receiver is placed on a fixed location. The BLE tracker is placed at different distances away from the receiver. At each distance, the tracker is rotated in four different angles of rotation: 0, 90, 180 and 270 degrees, and in two different orientations as seen in Fig. 3-5. Then, a set of RSSI values are collected from each rotating angle in each distance.

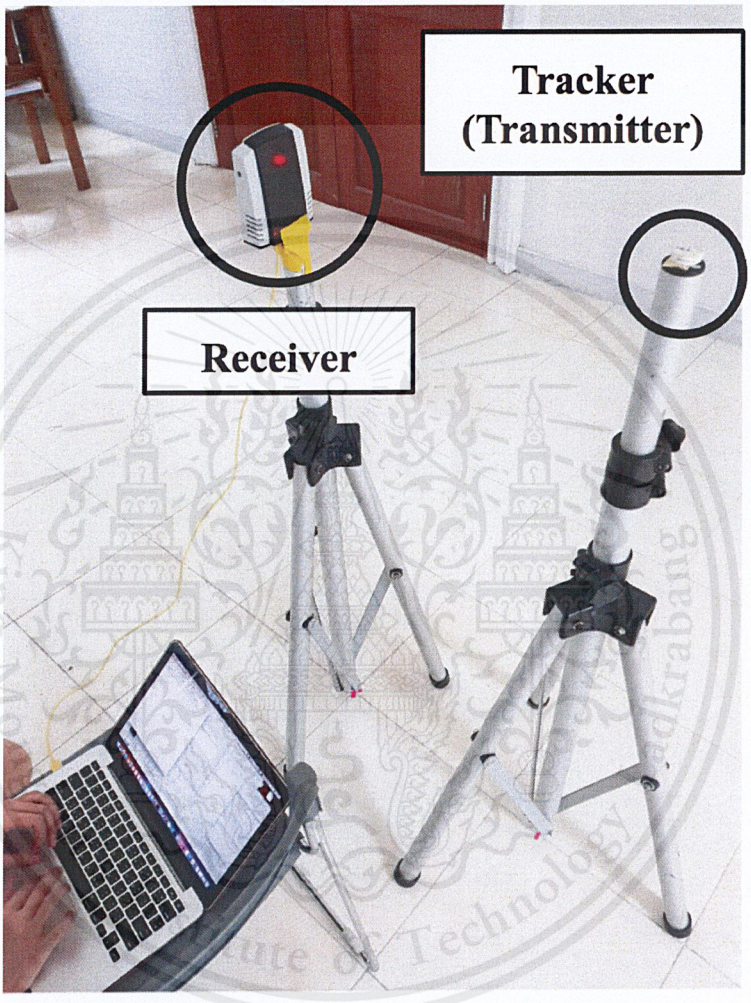


Figure 3-4: Setup of data collection

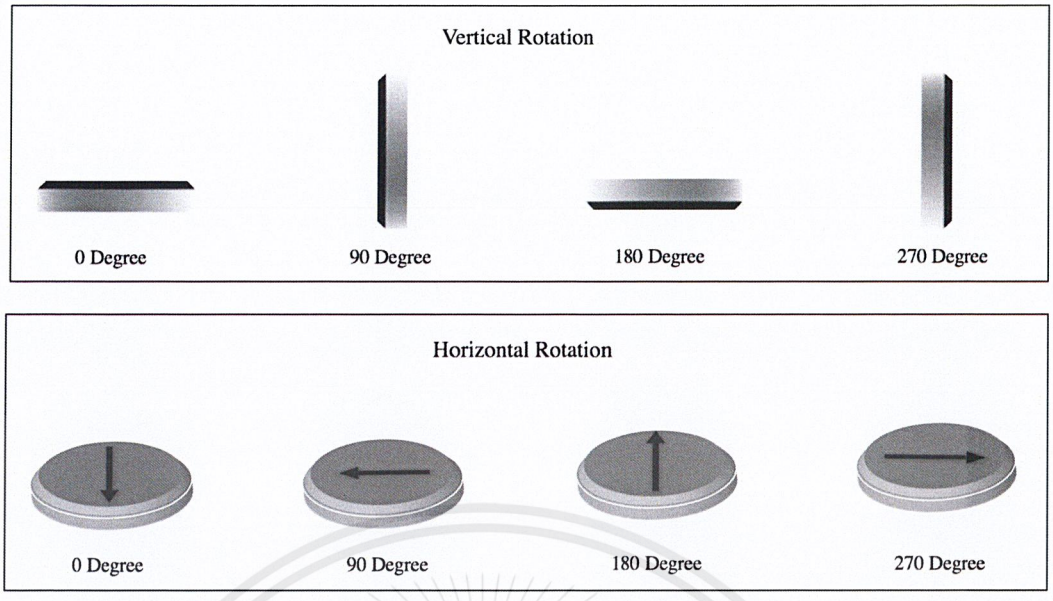


Figure 3-5: Vertical and Horizontal rotation of tracker.

### 3.1.2 Data Preprocessing

After collecting the raw RSSI data from data collection process, data preprocessing techniques are used for removing unnecessary data and smoothing the noisy data. Our raw data is an RSSI that is collected from the tracker (target object) using the receiver, with various angle of rotations of the tracker. This data fluctuates and contains outliers which could effect the accuracy of the system. In this thesis, three different data preprocessing techniques are applied on the RSSI data of a specific tracker orientation, namely, moving average, moving median and channel separation. The moving average and moving median techniques are used to filter out the outliers of the collected RSSI data, by calculating the mean and median of the RSSI data respectively over a specific window size. In addition, we propose the channel separation preprocessing technique that uses the clustering method in combination with moving average.

### Moving Average

Moving average or moving mean is a method to smooth out short-term fluctuations and highlight longer-term trends or cycles by creating series of averages of subset of the whole data set. First we decide on the window size (subset size i.e. window size = 20 meaning there are 20 in each subset). A good window size should be the size that give us small standard deviation and still realistically represent the trend of the data. Then we find the average of each window including the overlapped data as well.

Example:

$$\acute{y_1} = \frac{y_1 + y_2 + y_3 + ... + y_{(w+1)-1}}{w} \tag{3.1}$$

$$\acute{y_2} = \frac{y_2 + y_3 + y_4 + ... + y_{(w+2)-1}}{w} \tag{3.2}$$

Where $\acute{y_n}$ is the data in the filtered data set, $y_n$ is the data from the original set and $w$ is the window size. Since we are including the overlapped data, $\acute{y_2}$ will also include the original data at $y_2...y_{(w+1)-1}$ in the calculation even though $y_2...y_{(w+1)-1}$ is already included in the calculation of Eq. 3.1. After the process is done we will get a filtered data set $\acute{y}$ which has a significantly less standard deviation than the original data set $y$ thus having less noise.

### Moving Median

Similar to moving average, moving median is a method to reduce the noise in a data set, but instead of finding the mean in each window we use median. Moving median can be a better method of reducing noise in the cases such as rapid shocks or other anomalies that will cause the average to dramatically fluctuate.

Example:

$$\acute{y_1} = median(y_1 + y_2 + y_3 + ... + y_{(w+1)-1}) \tag{3.3}$$

### Deciding Window Size

In data filtering, a window size must be specified to the filtering process (e.g. moving average). A measurement called sum of absolute differences (SAD) can be used in deciding the window size. SAD is a measure of the similarity between image blocks in digital image processing. The lower the SAD, the more similar the image blocks are. SAD can be applied to measure the amount of shifts between original and filtered data, in other words how much the data changes after being filtered. Eq. (3.4) shows how to calculate the SAD

$$SAD = \sum_{i=1}^{n} |original_i - filtered_i| \tag{3.4}$$

where $i$ is the current index in the data vector and $n$ is the size of the data vector.

An approach to select the best window size is to plot the SAD against different window sizes as shown in Fig. 3-6. The x axis represents different window sizes of the moving average filtering method and y axis is the SAD obtained from performing moving average with a specific window size. In Fig. 3-6, notice that the SAD drops significantly in the beginning but stops decreasing and remain constant after window size of 20. It means that a window size over 20 won't have much effect on the data, so 20 is selected as the window size for this particular set of data.

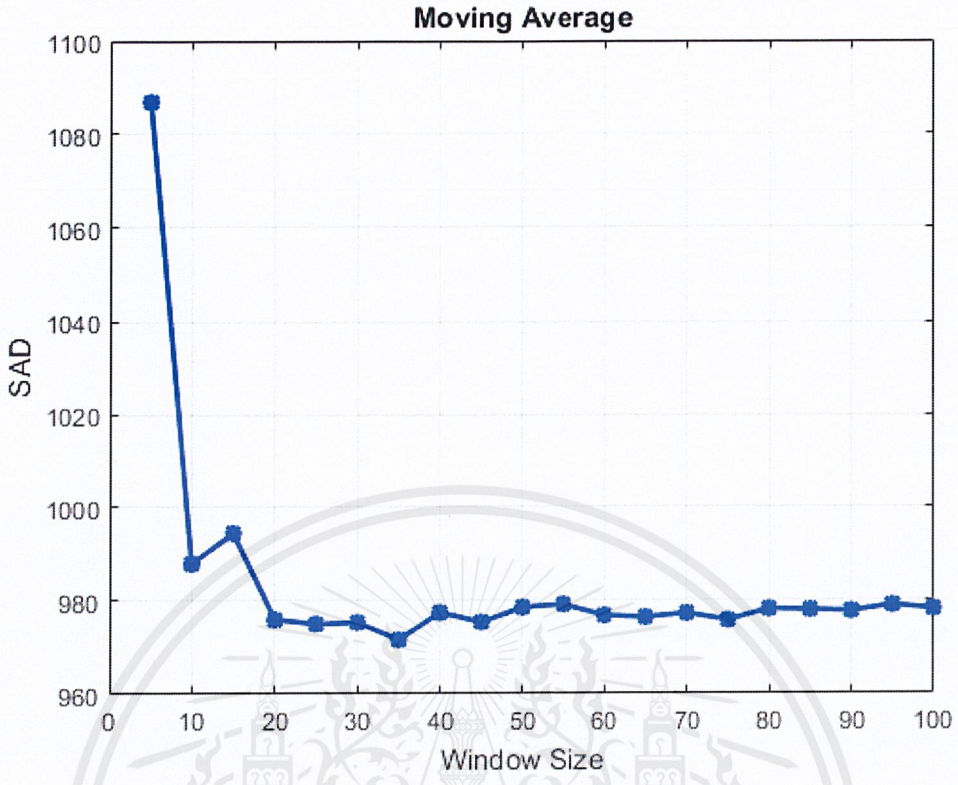


Figure 3-6: Graph of SAD vs. Window Size.

### Channel Separation

The BLE has 40 physical channels, three of which are used for broadcasting its advertising packets. Due to this nature of BLE, a channel separation preprocessing technique is used. The collected data is separated into three clusters for each advertising channel. K-means clustering is performed to distinguish which of the three channels the data belongs to. The top cluster represents channel 1 containing a set of highest RSSI values, the middle cluster for channel 2 and the bottom cluster for channel 3. For each channel, moving average is applied to smooth the series of data. In the end, we get 3 sets of filtered data (one from each channel).

### 3.1.3 Environmental Characterization

In this process, we are finding a model called the log-distance path loss model (or path loss model) for each tracker orientation using the data preprocessed by different preprocessing techniques. The log-distance path loss model is a radio propagation model that predicts the path loss or reduction in signal strength of a signal traveling in a given environment over distance, which can be used in indoor localization to find the distance given the signal strength. The propagation model in [18] shows that the average received signal strength decreases logarithmically with distance, which is where the name log-distance path loss model comes from. The actual equation of the model is shown below.

$$PL_{d_0 \to d} = PL_{d_0} + 10nlog_{10}(\frac{d}{d_0}) + X_\sigma \tag{3.5}$$

$PL_{d_0 \to d}$ represents the actual path loss of the signal at the target distance $d$ measured in dB. $PL_{d_0}$ is the path loss in decibel at reference distance $d_0$. $X_\sigma$ is a Gaussian random variable with zero mean. In a free space environment, this variable is zero. However in an obstructed environment, this random variable may have a value equals to the $\sigma$ standard deviation of a normal distribution caused by signal loss due to obstacles. Parameter $n$ is called the path loss exponent that can be calculated empirically, in prior, for each area which can vary approximately between 2 and 6, where 2 is in free space and 6 is in highly obstructed building [7].

The path loss of the signal tends to increase as the distance increases. In contrast, the RSSI is inversely related to the distance meaning it decreases as the distance increases. Since our thesis uses RSSI as the medium for localization, the equation can be rewritten as Eq. (3.6)

$$RSSI_d = RSSI_{d_0} - 10nlog_{10}(\frac{d}{d_0}) + X_\sigma \tag{3.6}$$

in which $RSSI_d$ represents the RSSI at the target distance $d$ measured in dB

and $RSSI_{d_0}$ is the RSSI measured at reference distance $d_0$ (where $d_0$ = 1 meter in our thesis).

In this process, the data of a specific tracker orientation preprocessed by the three preprocessing techniques in the previous process are being used. The median of the data preprocessed by moving median and the mean of the data preprocessed by moving average and channel separation are calculated for each distance then a method called curve fitting can be performed to determine the unknown value of $n$ that best suits the given dataset. Curve fitting is a method that constructs a curve or mathematical function that best fits a series of data points. In this thesis, Eq. (3.6) is used for curve fitting. The objective of this method is to find the value of $n$ that constructs a curve that has the lowest total sum of squared error (SSE), meaning the best fit to the series of data points. SSE measures the deviation between the expected data point and the predicted data point produced by the curve fitting method. An example of curve fitting using Eq. (3.6) to determine $n$ can be seen in Fig. 3-7. In this figure, Eq. (3.6) forms a curve that best fits this particular set of data points when $n$ is equal to 1.6842. Notice that the value of $n$ is close to 2 since the data is collected in a free space environment. The best fit curve represents the path loss model of the specific environment where the data is collected, the specific angle of the tracker and the specific preprocessing technique performed on the data (e.g. path loss model for free space area on KMITL 6th floor, 0 degree tracker's vertical rotating angle, data preprocessed by moving average with window size of 20).

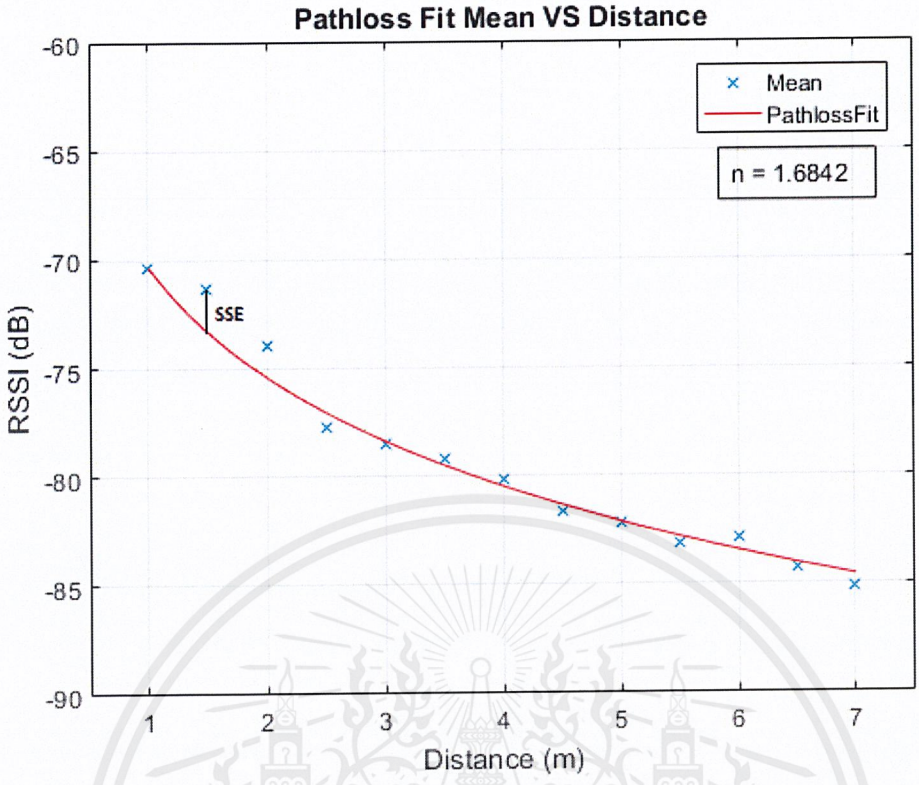


Figure 3-7: Example of Curve Fitting using Log-Distance Path Loss Equation.

## 3.2 Finding Object Location

### 3.2.1 RSSI-Distance Conversion (Distance Estimation)

In this process, the RSSI value is collected continuously by at least three receivers. The collected RSSI data is preprocessed by the three preprocessing techniques and substituted into the corresponding path loss model to determine the distance between the target object and each receiver. The equation of the path loss model can be rearranged to solve for the distance as in Eq. (3.7).

$$d = d_0 \cdot 10^{\frac{RSSI_d - RSSI_{d_0} - X_\sigma}{-10n}} \tag{3.7}$$

The $RSSI_{d_0}$ and $n$ is specific to each path loss model (determined in the

previous process), while the $RSSI_d$ is obtained from either the mean or median of the preprocessed test set (e.g. mean of data preprocessed by moving average and channel separation, median of data preprocessed by moving median).

### 3.2.2 Trilateration

Once we obtain the distances between the target object and each reference node as seen in Fig. 2-2, trilateration method can be applied to determine the exact location of the target object. Referring to Fig. 2-6, Eq. (3.8), Eq. (3.9) and Eq. (3.10) can be constructed according to the Euclidean distance formula.

$$d_1{}^2 = (x - x_1)^2 + (y - y_1)^2 \tag{3.8}$$

$$d_2{}^2 = (x - x_2)^2 + (y - y_2)^2 \tag{3.9}$$

$$d_3{}^2 = (x - x_3)^2 + (y - y_3)^2 \tag{3.10}$$

Simplifying the above equations through several mathematical operations produce the following Eq. (3.11) and Eq. (3.12), where Eq. (3.11) is used to find the x coordinate of the target object and Eq. (3.12) is for the y coordinate.

$$A = -2x_1 + 2x_2$$

$$B = -2y_1 + 2y_2$$

$$C = d_1{}^2 - d_2{}^2 - x_1{}^2 + x_2{}^2 - y_1{}^2 + y_2{}^2$$

$$D = -2x_2 + 2x_3$$

$$E = -2y_2 + 2y_3$$

$$F = d_2{}^2 - d_3{}^2 - x_2{}^2 + x_3{}^2 - y_2{}^2 + y_3{}^2$$

$$x = \frac{CE - FB}{EA - BD} \tag{3.11}$$

$$y = \frac{CD - AF}{BD - AE} \tag{3.12}$$

Knowing the coordinates of the three reference nodes (i.e. $(x_1, y_1)$, $(x_2, y_2)$, $(x_3, y_3)$) and the distances between the target node and the reference nodes (i.e. $d_1$, $d_2$, $d_3$), these known values can be substituted into the equation to obtain the x and y coordinate of the target node.

# Chapter 4

# Experiments

Data preprocessing can affect the accuracy of distance estimation. In this section, we explore the effect of different preprocessing techniques on distance estimation performance.

## 4.1 Datasets

In our experiments, all RSSI datasets are collected in an open area inside the 6th floor of the International College building in King Mongkut's Institute of Technology Ladkrabang (KMITL) at 4 different angle of rotations of the tracker (e.g. angle 0, 90, 180, 270) with no obstacles between tracker and receiver.

**Training Sets**

Following is the list of all datasets we collected using B4 Bracelet Beacon and BLE Anchor:

1. Dataset 1 – 200 samples, 2 distances (e.g. 2, 4), collected at International College 6th floor in KMITL on September 28, 2017. This dataset only contains 1 angle (0 degree) and 3 different sampling rates (e.g. 1, 2, 10 Hz), to test the effect of sampling rates on RSSI.

2. Dataset 2 – 500 samples, 8 distances (e.g. 0.5, 1, 2 ...7), collected on October 10, 2017.

3. Dataset 3 – 500 samples, 8 distances (e.g. 0.5, 1, 2 ...7), collected on October 23, 2017.

4. Dataset 4 – 200 samples, 14 distances (e.g. 0.5, 1, 1.5 ...7), collected on October 24, 2017.

Following is the list of all datasets we collected using AiR Node and Raspberry Pi 3 Receiver:

1. Dataset 5 – 200 samples, 14 distances (e.g. 0.5, 1, 1.5 ...7), collected on January 13, 2018.

2. Dataset 6 – 200 samples, 14 distances (e.g. 0.5, 1, 1.5 ...7), collected on February 20, 2018.

3. Dataset 7 – 200 samples, 14 distances (e.g. 0.5, 1, 1.5 ...7), collected on April 20, 2018.

**Test Sets**

Following is the list of all datasets we collected using AiR Node and Raspberry Pi 3 Receiver:

1. Dataset 8 – 200 samples, 14 distances (e.g. 0.5, 1, 1.5 ...7), collected on March 7, 2018.

## 4.2 Measures

The main statistical measures that we use to evaluate the performance of our system are the minimum absolute error, maximum absolute error, standard deviation of the absolute errors and the Root Mean Squared Error (RMSE). The absolute error measures the absolute difference between the expected and the

actual result. RMSE basically measures the average of the differences between the expected and the actual results, calculated by Eq. (4.1) below

$$RMSE = \sqrt{\frac{1}{n}\sum_{i=1}^{n}(y_i - \hat{y}_i)^2} \tag{4.1}$$

where $n$ is the number of predictions, $y$ is the vector of expected values and $\hat{y}$ is the vector of actual values being predicted.

## 4.3 Experiments

We conducted several experiments on all of our datasets to study the nature of the data and formulate hypotheses. In this section, we present the main experiments on a specific dataset where we explore different factors that can affect the performance of the system. Since the antenna of the tracker broadcasts the signal as a donut-shaped, rotating the tracker horizontally has no significant effect on the RSSI. Therefore, this section only focuses on the vertical rotation of the BLE tracker.

### 4.3.1 Experiment 1: Effects of Vertical Rotation of BLE tracker

#### Objective

The experiment was conducted to analyze the effects of vertical rotation of the BLE tracker on the values of RSSI.

#### Experimental Procedure

Dataset 6 is used in this experiment. Matlab is used to obtain the path loss models by fitting a curve through the distance-specific means of Dataset 6 for each device orientation.

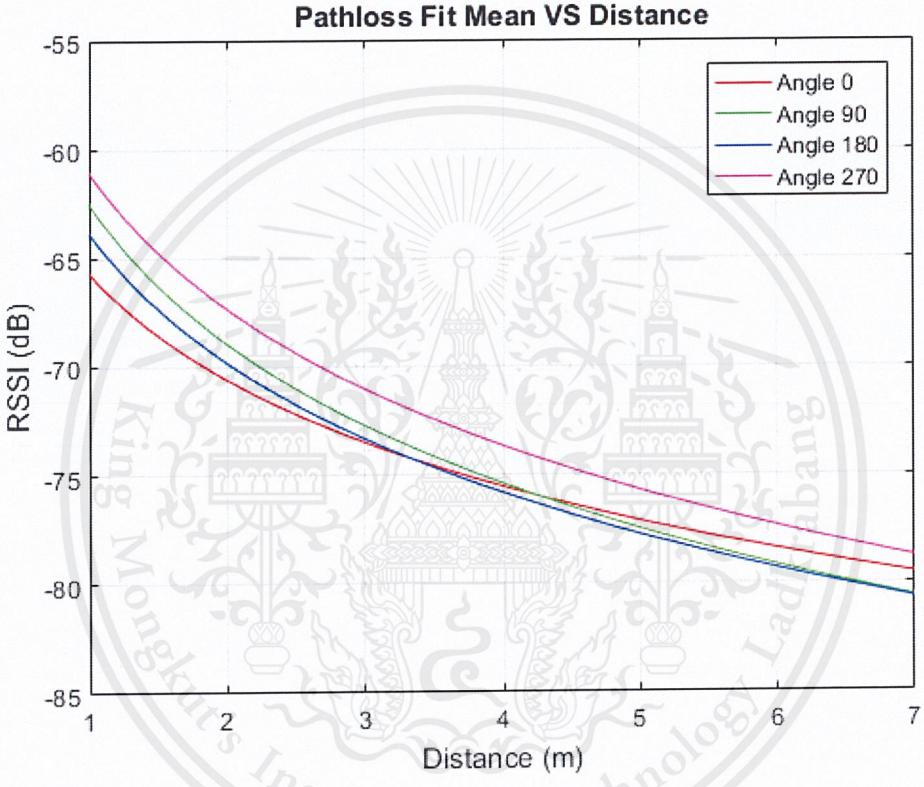


Figure 4-1: Curve Fitting of All Angles

**Result**

Fig. 4-1 illustrates the path loss models of 4 different device orientation on the same graph. The result implies that vertical rotation of the BLE tracker can systematically affect the RSSI values. Angle 0 has lowest signal strength, followed by angles 180, 90 and 270, respectively. After 2.5 meters, the curve for Angle 0 starts to overlap with the curves of angle 90 and angle 180. This could be due to the degradation of signal strength as the distance increases, thus the signal is less stable. Incorporating the device orientation information into the path loss model, therefore, are likely to improve the distance estimation accuracy.

### 4.3.2 Experiment 2: Preprocessing by Mean

**Objective**

This experiment is conducted to observe the effectiveness of data preprocessing based on the means of the RSSI data and to visualize the path loss model obtained from the means of RSSI data.

**Experimental Procedure**

We tried to apply moving average filter with a window size of 20 using Matlab on Dataset 6 for all 4 angles of vertical rotation to smooth the RSSI readings. Then, curve fitting is performed on the means of the filtered data to obtain the path loss model.

**Result**

Fig. 4-2 shows an example of the plot of raw RSSI samples at distance of 2 meters and the RSSI samples after being filtered by moving average of window size 20. We can see the filtered data becomes smoother and less scattered.

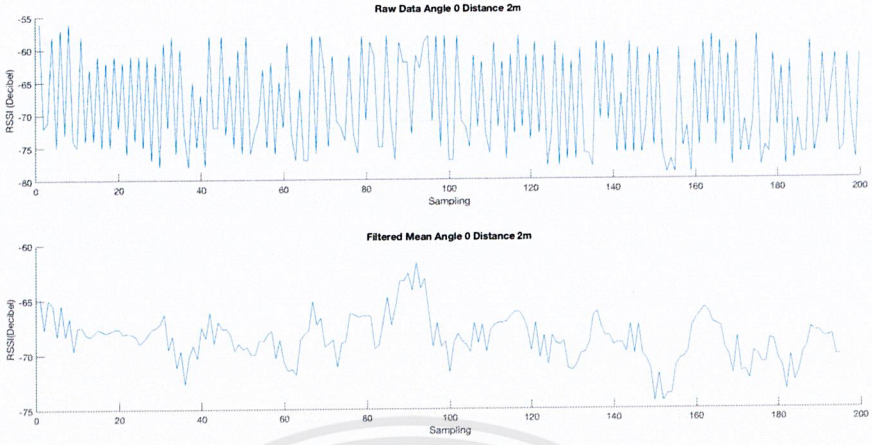


Figure 4-2: Raw Data vs Data filtered by Moving Average (Angle 0 at 2 meters)

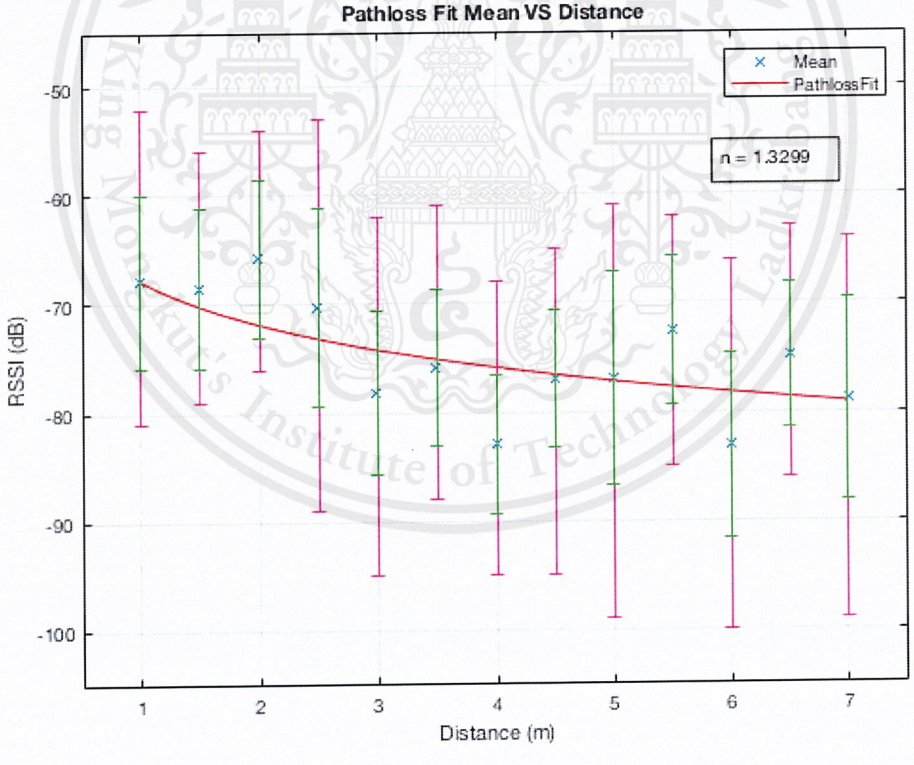


Figure 4-3: Curve Fitting of Raw Data using Mean (Angle 0)

Fig. 4-3 is the path loss model resulted from the curve fitting of the means of raw RSSI data of angle 0. The path loss exponent of the path loss model achieved from this dataset is 1.3299. The green error bars on the data points represents the standard deviation of the data at that distances, while the pink error bar represents the min-max error bar.

Fig. 4-4 is the path loss model resulted from the curve fitting of the means of filtered RSSI data of angle 0 by moving average. The path loss exponent of the path loss model achieved from this dataset is 1.3308. Notice that the SD and min-max error bars greatly reduced compared to the error bars in Fig. 4-3.

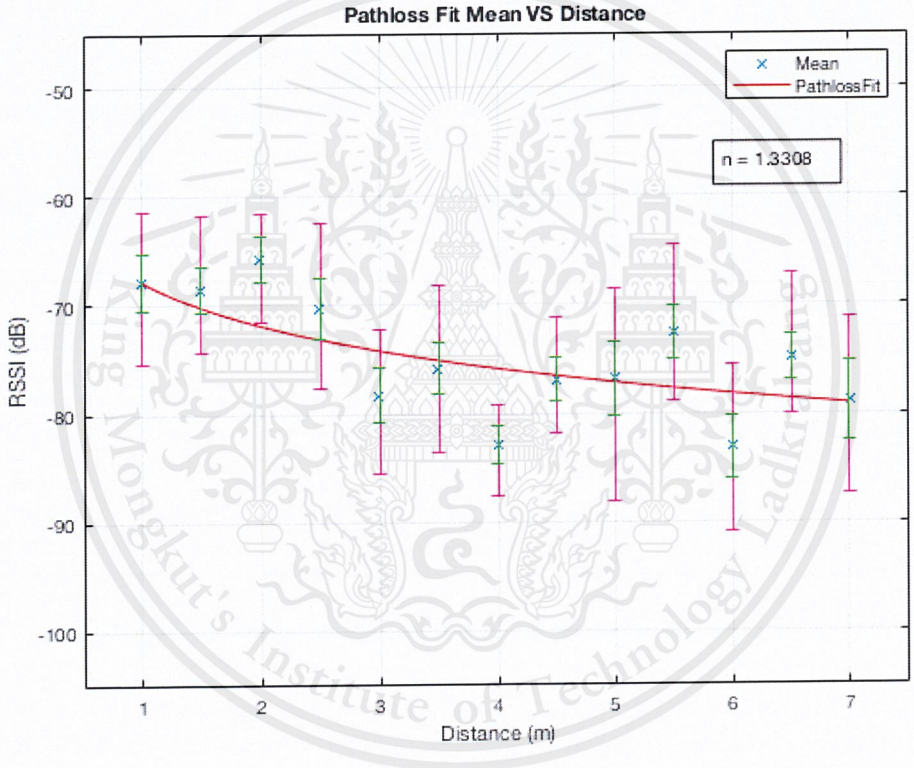


Figure 4-4: Curve Fitting of Filtered Data by Moving Average (Angle 0)

Table 4.1 summarizes the basic statistics of the data filtered by moving average at multiple distances.

Table 4.1: Summary Statistics of Moving Average.

| Distance | Mean | Median | Mode | SD |
|---|---|---|---|---|
| 0.5 m | -62.597 | -62.500 | -67.500 | 2.855 |
| 1 m | -67.839 | -68.000 | -65.333 | 2.548 |
| 1.5 m | -68.562 | -68.500 | -68.333 | 2.114 |
| 2 m | -65.780 | -65.333 | -64.667 | 2.119 |
| 2.5 m | -70.268 | -70.333 | -69.667 | 2.758 |
| 3 m | -78.269 | -78.167 | -80.833 | 2.517 |
| 3.5 m | -75.858 | -76.167 | -77.833 | 2.356 |
| 4 m | -82.886 | -83.000 | -82.833 | 1.700 |
| 4.5 m | -76.874 | -76.667 | -76.667 | 2.004 |
| 5 m | -76.816 | -76.833 | -77.500 | 3.442 |
| 5.5 m | -72.510 | -72.667 | -72.833 | 2.439 |
| 6 m | -83.074 | -82.833 | -85.333 | 2.909 |
| 6.5 m | -74.789 | -75.000 | -75.167 | 2.114 |
| 7 m | -78.893 | -78.667 | -80.000 | 3.656 |

### 4.3.3 Experiment 3: Preprocessing by Median

**Objective**

This experiment is conducted to observe the effectiveness of data preprocessing based on the medians of the RSSI data and to visualize the path loss model obtained from the medians of RSSI data.

**Experimental Procedure**

We tried to apply moving median filter with a window size of 20 using Matlab on Dataset 6 for all 4 angles of vertical rotation to smooth the RSSI readings. Then, curve fitting is performed on the medians of the filtered data to obtain the path loss model.

**Result**

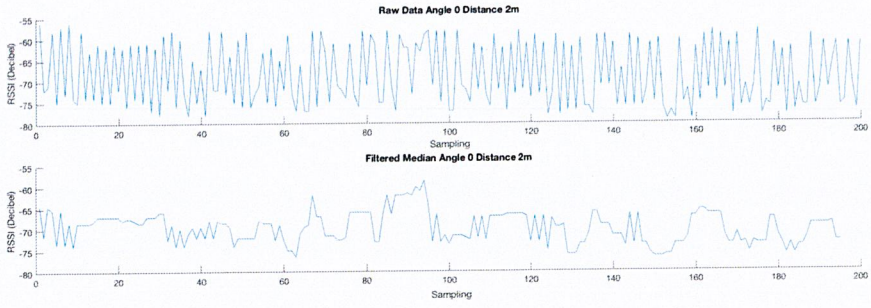


Figure 4-5: Raw Data vs Data filtered by Moving Median (Angle 0 at 2 meters)

Fig. 4-5 shows an example of the plot of raw RSSI samples at distance of 2 meters and the RSSI samples after being filtered by moving median of window size 20.

Fig. 4-6 is the path loss model resulted from the curve fitting of the medians of raw RSSI data of angle 0. The path loss exponent of the path loss model achieved from this dataset is 1.3506. The green error bars on the data points represents the standard deviation of the data at that distances, while the pink error bar represents the min-max error bar.

Fig. 4-7 is the path loss model resulted from the curve fitting of the medians of filtered RSSI data of angle 0 by moving median. The path loss exponent of the path loss model achieved from this dataset is 1.1745. the SD and min-max error bars reduce but the SD is still higher than the SD of data filtered by moving average in Fig. 4-4. Notice that the fitted curve or the path loss model becomes flat and the path loss exponent $n$ decreases, resulting from the changes in the medians of the filtered data from the raw data. From these information, we conclude that moving median is not a suitable preprocessing technique for our dataset.

Table 4.2 summarizes the basic statistics of the data filtered by moving median at multiple distances.

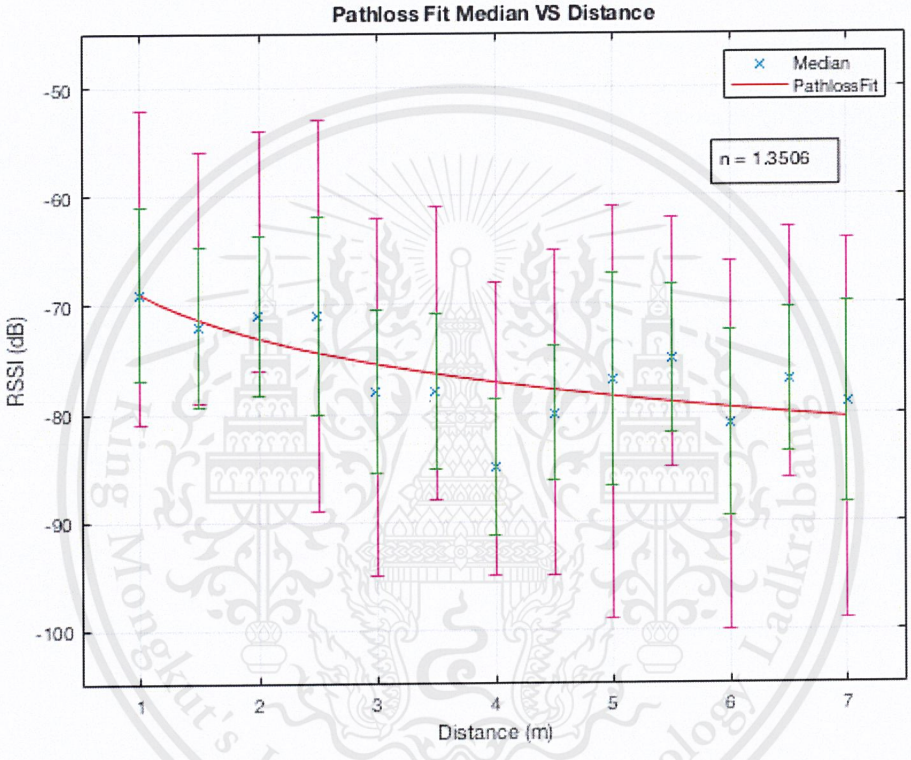


Figure 4-6: Curve Fitting of Raw Data using Median (Angle 0)

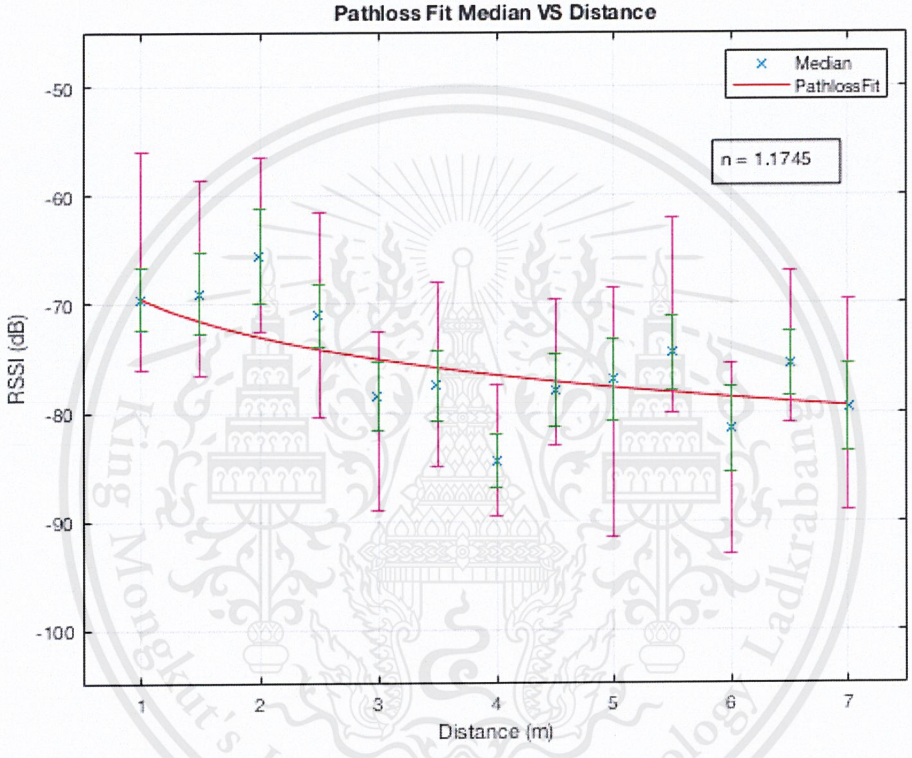


Figure 4-7: Curve Fitting of Filtered Data by Moving Median (Angle 0)

Table 4.2: Summary Statistics of Moving Median.

| Distance | Mean | Median | Mode | SD |
|---|---|---|---|---|
| 0.5 m | -64.308 | -64.000 | -69.000 | 4.276 |
| 1 m | -69.249 | -69.500 | -70.500 | 2.953 |
| 1.5 m | -69.744 | -69.000 | -67.000 | 3.714 |
| 2 m | -66.877 | -65.500 | -71.000 | 4.355 |
| 2.5 m | -70.490 | -71.000 | -71.000 | 2.886 |
| 3 m | -79.028 | -78.500 | -78.000 | 3.113 |
| 3.5 m | -77.126 | -77.500 | -78.000 | 3.227 |
| 4 m | -84.074 | -84.500 | -86.000 | 2.441 |
| 4.5 m | -78.090 | -78.000 | -81.000 | 3.325 |
| 5 m | -77.256 | -77.000 | -77.000 | 3.714 |
| 5.5 m | -73.408 | -74.500 | -76.000 | 3.434 |
| 6 m | -83.123 | -81.500 | -80.500 | 3.922 |
| 6.5 m | -75.410 | -75.500 | -78.000 | 2.962 |
| 7 m | -78.864 | -79.500 | -80.000 | 4.026 |

### 4.3.4 Experiment 4: Preprocessing by Channel Separation

**Objective**

This experiment is conducted to obtain channel-specific path loss models through data preprocessing by BLE channel separation technique in combination with moving average.

**Experimental Procedure**

We propose a preprocessing approach that separately computes the path loss model for each advertising channel. We perform K-means clustering to be able to distinguish which data belongs to which of the 3 channels. For each channel,

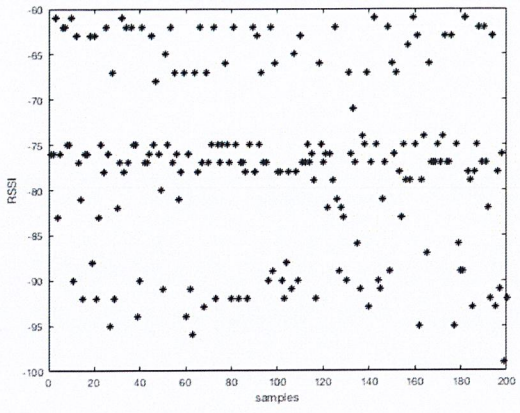


(a) Scatter Plot

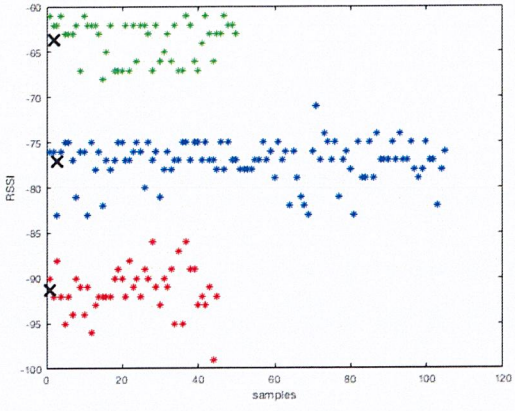


(b) K-means Clustering (k = 3)

Figure 4-8: Raw Data of Angle 0 at 5 m

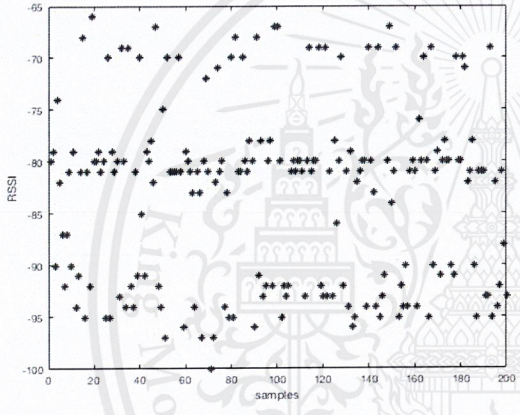


(a) Scatter Plot

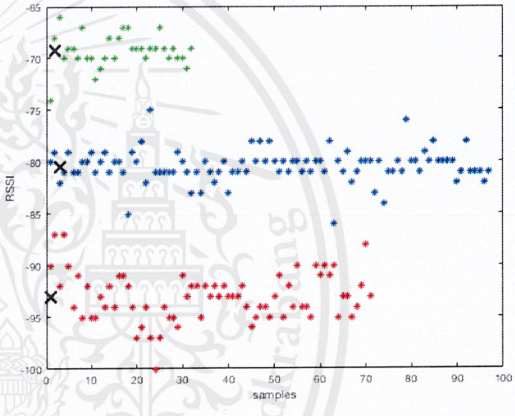


(b) K-means Clustering (k = 3)

Figure 4-9: Raw Data of Angle 0 at 6 m

we apply moving average and find the mean of the set of RSSI of each distance then apply curve fitting to obtain the path loss model.

**Result**

Fig. 4-8a is an example of a scatter plot of the raw RSSI data of angle 0 at 5 meters. Fig. 4-8b is the result of K-means clustering of the raw data resulting in 3 clusters, each cluster represents an advertising channel of BLE device. Similarly in Fig. 4-9, the raw data collected can be separated into 3 clusters. The green

cluster is assumed to be channel 1 or the channel containing the highest values of RSSI. The blue cluster is assumed to be channel 2 or the channel with the second highest values of RSSI. Finally, the red cluster is assumed to be channel 3 or the channel with the lowest values of RSSI.

Fig. 4-10 is the path loss model resulted from the curve fitting of the mean of raw RSSI data of angle 0 in channel 1. The path loss exponent of the path loss model achieved from this dataset is 1.4317. the SD error bar in green is significantly low due to the low number of clustered data in channel 1.

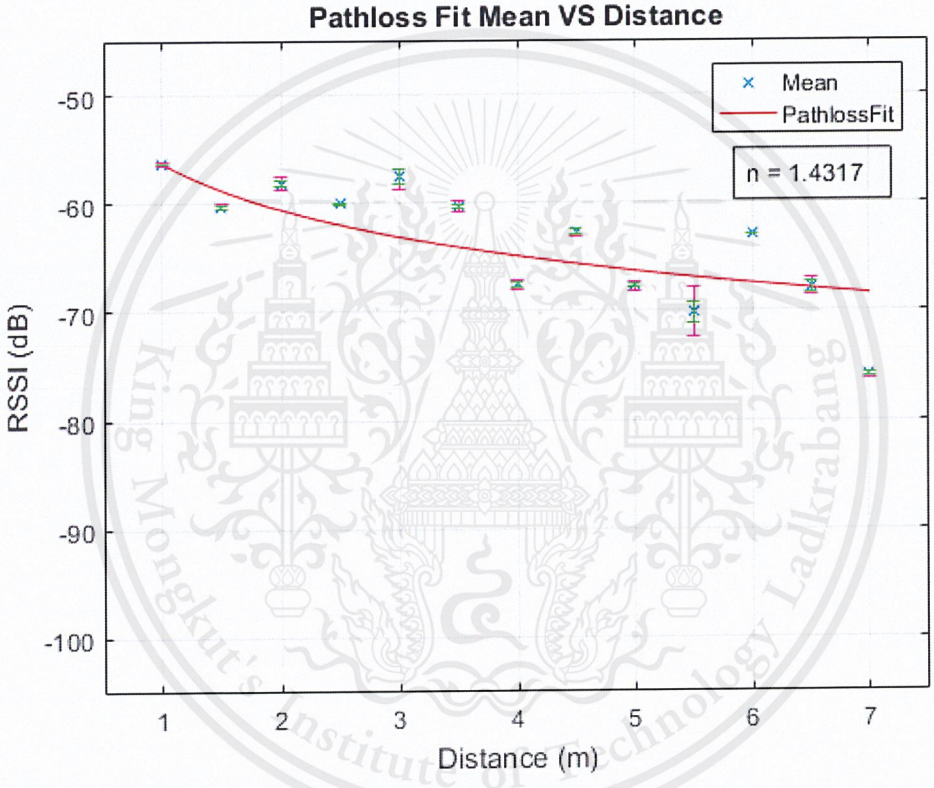


Figure 4-10: Curve Fitting of Channel 1 using Mean (Angle 0)

Fig. 4-11 is the path loss model resulted from the curve fitting of the mean of raw RSSI data of angle 0 in channel 2. The path loss exponent of the path loss model achieved from this dataset is 2.7101.

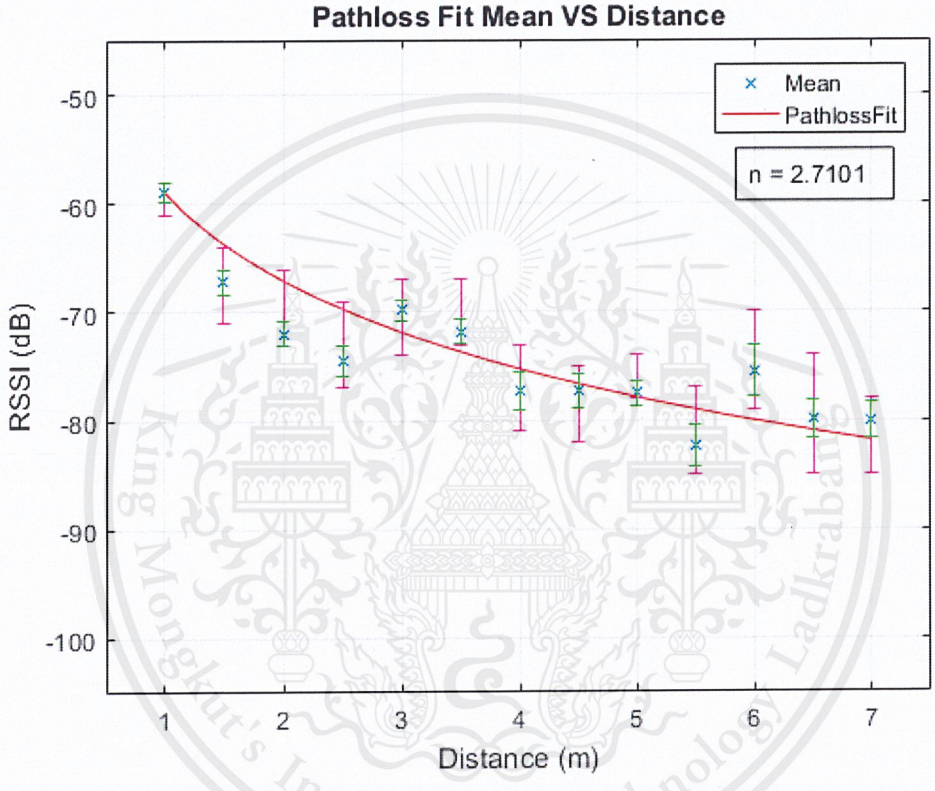


Figure 4-11: Curve Fitting of Channel 2 using Mean (Angle 0)

Fig. 4-12 is the path loss model resulted from the curve fitting of the mean of raw RSSI data of angle 0 in channel 3. The path loss exponent of the path loss model achieved from this dataset is 1.9897.

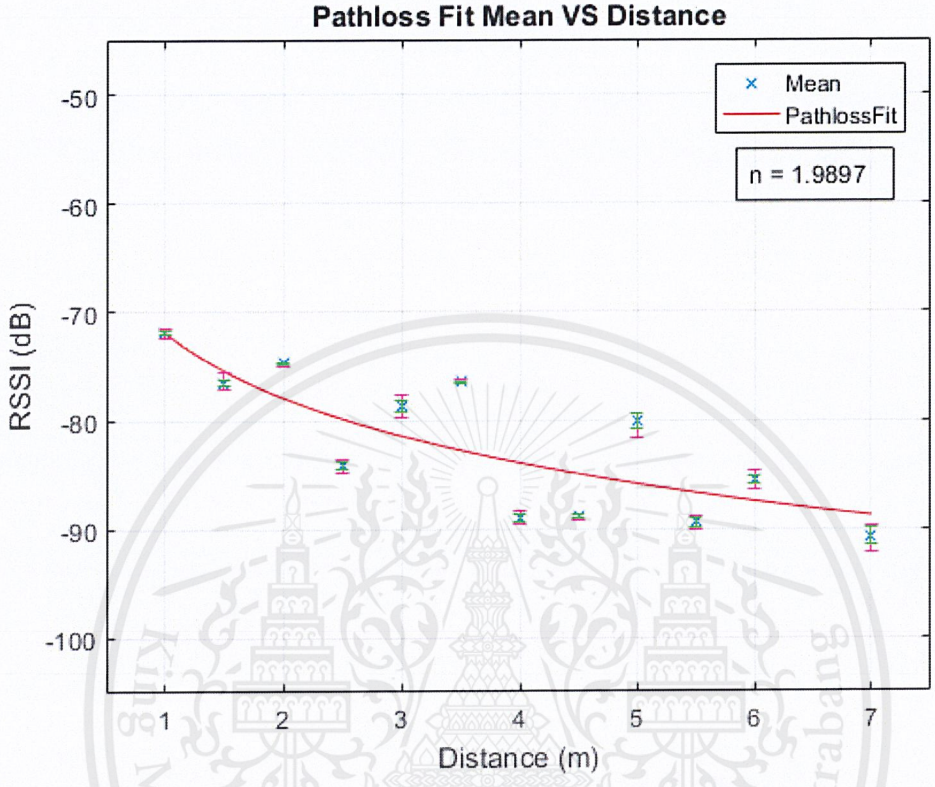


Figure 4-12: Curve Fitting of Channel 3 using Mean (Angle 0)

### 4.3.5 Experiment 5: Distance Estimation of Angle 0

**Objective**

This experiment is conducted to evaluate the performance of distance estimation by the path loss models obtained from 3 different preprocessing techniques: moving average, moving median and the channel separation technique. The experiment also compares the performance of distance estimation by known tracker orientation against unknown tracker orientation.

**Experimental Procedure**

The test set containing the data of angle 0 from Dataset 8 is being used to do distance estimation by using the models presented earlier. Since device orientation can affect the accuracy, the experiment is performed to compare the estimation results based on the data extracted from a known device orientation (Angle 0) and unknown device orientation (all angles). The test dataset is preprocessed by the aforementioned technique before substituting into the corresponding path loss model to obtain the distance. For preprocessing with channel separation, the test data is first separated into three clusters by K-means clustering and each cluster is further filtered by moving average prior to distance estimation. In this study, a fixed window size of 20 samples and a shifted window of size 1 are used.

**Result**

Table 4.3 shows a performance comparison among different preprocessing techniques based on RMSE, minimum absolute error, maximum absolute error and the standard deviation (SD) of the absolute errors. The RMSE of distance estimation with moving average is 1.599 for unknown device orientation, and slightly reduces to 1.477 for known device orientation (Angle 0). Preprocessing by moving median for known device orientation yields a higher RMSE of 1.94. Since moving average outperforms moving median, we apply moving average to the data of each channel obtained from channel separation. As a result, estimation by channel 1, channel 2 and channel 3 with known device orientation yields RMSE of 1.401, 1.194 and 1.67, respectively. The channel separation preprocessing technique indeed improves the accuracy of the distance estimation except for channel 3, where channel 2 has the lowest RMSE, maximum error and SD of absolute errors among all channels in this experiment.

Table 4.3: Result of distance estimation

| **Pre-processing Techniques** | **Angle 0** | | | | **Unknown Angle** | | | |
|---|---|---|---|---|---|---|---|---|
| | RMSE | Minimum absolute error | Maximum absolute error | SD | RMSE | Minimum absolute error | Maximum absolute error | SD |
| Moving Average | 1.477 | 0.011 | 5.562 | 1.069 | 1.599 | 0.003 | 7.633 | 1.165 |
| Moving Median | 1.940 | 0 | 9.106 | 1.488 | 2.660 | 0 | 20.08 | 2.144 |
| Channel 1 | 1.401 | 0.012 | 2.544 | 0.783 | 1.626 | 0.010 | 7.166 | 1.082 |
| Channel 2 | 1.194 | 0.025 | 2.372 | 0.713 | 1.400 | 0.011 | 3.634 | 0.835 |
| Channel 3 | 1.670 | 0.001 | 4.805 | 1.168 | 1.821 | 0.001 | 6.284 | 1.265 |

Fig. 4-13 shows the bar graph of RMSE resulted from the distance estimation based on channel 2 preprocessing versus different distances. The error bar indicates the resulting minimum and maximum absolute errors. Notice that apart from 2.5 meters and from 5 to 6 meters, the RMSE from the distance estimation with known angle (shown in red) are lower than the RMSE from unknown angle (shown in green). Distance estimation with unknown angle tends to produce error bars with larger range and higher maximum absolute errors. This implies that distance estimation with unknown device orientation produce a more scattered and less reliable output. In addition, we can see that the unknown angle model unexpectedly produces a lower error when the distance is beyond 4.5 meters, which believe to be caused by signal degradation. Thus, setting the receiver within a 4 meter range from the tracker seems to be a good option for the environmental setup.

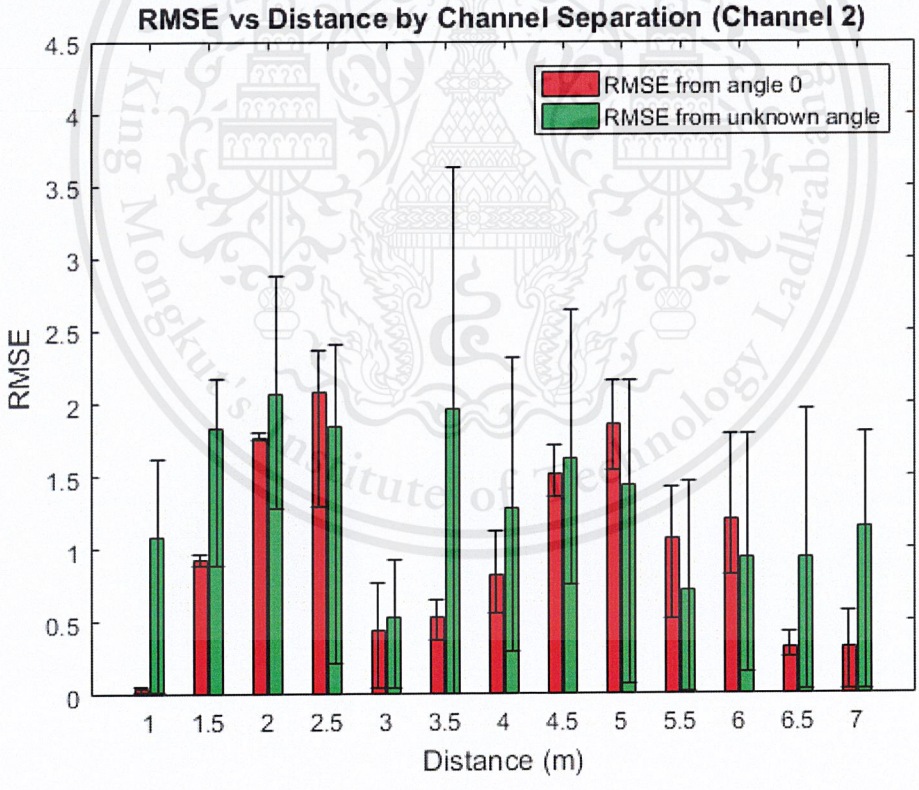


Figure 4-13: RMSE of Distance Estimation by Channel Separation Preprocessing (Channel 2)

According to the results, channel 2 preprocessing with known device orientation achieves an RMSE of 1.194 and SD of 0.713. This illustrates that choosing the correct channels for distance estimation and device orientation information can effectively improve the performance of the system.

### 4.3.6 Experiment 6: Trilateration of Angle 0

#### Objective

This experiment is conducted to evaluate the performance of trilateration by the path loss models of known angle (angle 0) obtained from 2 different preprocessing techniques: moving average with window size of 20 and the channel separation technique.

#### Experimental Procedure

The training set containing the data of angle 0 from Dataset 7 is being preprocessed by the 2 preprocessing techniques mentioned above and then applied curve fitting to create path loss models.

The test sets of 200 samples of RSSI are collected real-time by each receiver, before being preprocessed by two different preprocessing techniques and substituted into the path loss models to obtain the distances then applied the trilateration equation to get the position of the target object. Only three receivers closest to the tracker (target object) will be used for trilateration. Fig. 4-14 shows how the devices are set up for the trilateration experiment.

**Result**

Table 4.4 shows a performance comparison between moving average and channel separation of known angle (angle 0) at position (1,3) based on Root Mean Squared Error (RMSE), minimum absolute error, maximum absolute error and the standard deviation (SD) of the absolute errors. The RMSE of trilateration with moving average is 1.098, while channel separation with channel 3 achieves a lower RMSE of 0.730. For raw trilateration results and absolute errors of position (1,3), see Appendix A.1.

Table 4.4: Statistics of trilateration result of position 1,3.

| | **Moving Average** | **Channel 1** | **Channel 2** | **Channel 3** |
|---|---|---|---|---|
| RMSE | 1.098 | 1.155 | 1.348 | 0.730 |
| Min Abs Error | 0.882 | 0.721 | 1.218 | 0.338 |
| Max Abs Error | 1.220 | 1.648 | 1.400 | 1.045 |
| SD | 0.132 | 0.335 | 0.074 | 0.252 |

Table 4.5 shows a performance comparison between moving average and channel separation of known angle (angle 0) at position (1,1). The RMSE of trilateration with moving average is 0.709, while channel separation with channel 1 achieves a slighty lower RMSE of 0.702. For raw trilateration results and absolute errors of position (1,1), see Appendix A.2.

Table 4.5: Statistics of trilateration result of position 1,1.

| | **Moving Average** | **Channel 1** | **Channel 2** | **Channel 3** |
|---|---|---|---|---|
| RMSE | 0.709 | 0.702 | 1.705 | 0.863 |
| Min Abs Error | 0.598 | 0.629 | 0.950 | 0.834 |
| Max Abs Error | 0.824 | 0.810 | 2.125 | 0.891 |
| SD | 0.083 | 0.074 | 0.477 | 0.021 |

Table 4.6 shows a performance comparison between moving average and

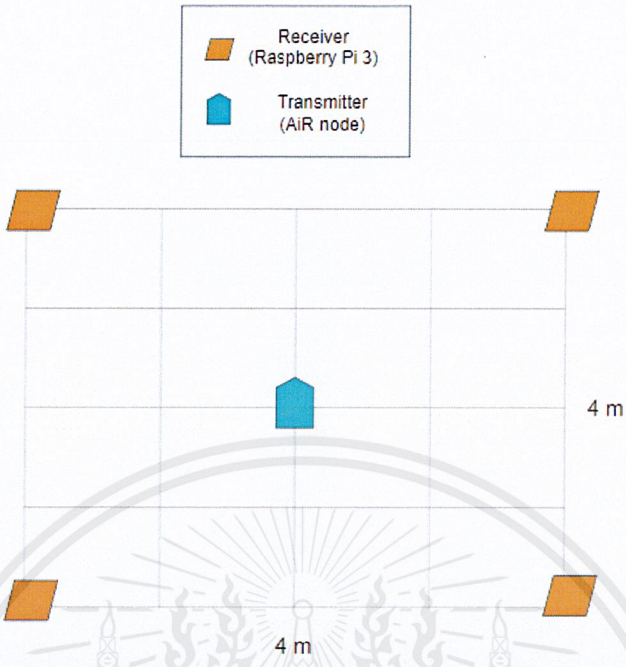


(a) Overview of Trilateration Setup

(b) Trilateration Setup on 6th Floor of KMITL

Figure 4-14: Setup of Trilateration

channel separation of known angle (angle 0) at position (2,1). The RMSE of trilateration with moving average is 0.690, while channel separation with channel 1 achieves a slighty lower RMSE of 0.569. For raw trilateration results and absolute errors of position (2,1), see Appendix A.3.

Table 4.6: Statistics of trilateration result of position 2,1.

| | **Moving Average** | **Channel 1** | **Channel 2** | **Channel 3** |
|---|---|---|---|---|
| RMSE | 0.690 | 0.569 | 1.056 | 0.773 |
| Min Abs Error | 0.480 | 0.272 | 0.605 | 0.701 |
| Max Abs Error | 0.954 | 0.875 | 1.369 | 0.980 |
| SD | 0.181 | 0.249 | 0.284 | 0.120 |

Table 4.7 shows a performance comparison between moving average and channel separation of known angle (angle 0) at position (3,3). The RMSE of trilateration with moving average is 0.830, while channel separation achieves its lowest RMSE of 0.919 in channel 1. For raw trilateration results and absolute errors of position (3,3), see Appendix A.4.

Table 4.7: Statistics of trilateration result of position 3,3.

| | **Moving Average** | **Channel 1** | **Channel 2** | **Channel 3** |
|---|---|---|---|---|
| RMSE | 0.830 | 0.919 | 1.378 | 1.027 |
| Min Abs Error | 0.700 | 0.825 | 1.220 | 1.010 |
| Max Abs Error | 0.920 | 0.949 | 1.851 | 1.041 |
| SD | 0.082 | 0.052 | 0.277 | 0.011 |

Table 4.8 shows a performance comparison between moving average and channel separation of known angle (angle 0) at position (2,2). Trilateration with moving average achieves an RMSE as low as 0.173, while channel separation with channel 3 achieves a slighty lower RMSE of 0.154. For raw trilateration results and absolute errors of position (2,2), see Appendix A.5.

Table 4.8: Statistics of trilateration result of position 2,2.

| | **Moving Average** | **Channel 1** | **Channel 2** | **Channel 3** |
|---|---|---|---|---|
| RMSE | 0.173 | 0.468 | 0.521 | 0.154 |
| Min Abs Error | 0.108 | 0.396 | 0.156 | 0.050 |
| Max Abs Error | 0.230 | 0.532 | 1.004 | 0.194 |
| SD | 0.054 | 0.049 | 0.335 | 0.066 |

As a result, trilateration by known angle using the channel separation technique can achieve an RMSE as low as 0.173. However, the performance difference between moving average and channel separation is small. Furthermore, the error of each channel changes significantly in different experiments, indicating that the system may have to switch between channels to get the best result from trilateration.

# Chapter 5

# Conclusion

In this thesis, we studied the effect of tracker orientation and the different BLE advertising channels on the signal strength. A BLE channel separation pre-processing technique is proposed. By comparing the path loss models from the means of RSSI collected through 4 different angles of rotations for different distances, we see a systematic change in the RSSI values. Using the channel separation technique, we obtain a lower RMSE and SD of the estimation errors compared to the conventional method that uses moving average and moving median filtering. Furthermore, using channel separation with known angle of BLE tracker produces better results than unknown angle. From the results, we conclude that a combined use of channel separation with device orientation information can improve the distance estimation performance of BLE-based indoor localization by achieving an RMSE of 1.194 and SD of 0.713, and achieving an RMSE as low as 0.154 for trilateration.

## 5.1 Problems and Obstacles

### 5.1.1 Hardware limitation

For BLE devices, the device's battery has an effect to the RSSI. When the battery is low, the RSSI values drop causing a higher error on distances estimation.

Another problem for BLE device is that the environmental factors such as objects or people in the area could affect the BLE signal transmission which also lead to wrong distances estimation.

## 5.2 Future Work

### 5.2.1 Application

Deployed in a hospital or elderly care facilities, the mobile application can be improved to detect patient's sudden drop and the location where it happens. Furthermore, instead of assuming predefined beacon orientation in the program, the beacon equipped with accelerometer can send the angle of rotation to the receiver, so that the application can automatically choose the correct path loss model based on the corresponding beacon orientation.

### 5.2.2 Algorithm

Apart from moving average, there are several more preprocessing algorithms that can be used to further improve the localization performance. One of which is the Kalman filtering technique. An example of its application is shown by Ozer and John [1] using Kalman Filtering to produce smooth RSSI readings while maintaining quick response time.

# Bibliography


[1] O. Adrian and J. Eugene. Improving the accuracy of bluetooth low energy indoor positioning system using kalman filtering. In *2016 International Conference on Computational Science and Computational Intelligence*, 2016.

[2] T. ALice. Indooratlas hopes to unlock the "holy grail of advertising" with magnetic-field mapping, 2013.

[3] C. Chanaphon and P. Punyanuch. *Camfinder: Image-Based Indoor Positioning System*. PhD thesis, King Mongkut's Institute of Technology Ladkrabang, 2014.

[4] Y. Chouchang and S. Huai-rong. Wifi-based indoor positioning. *IEEE Communications Magazine*, 53:150–157, 2015.

[5] P. Chuan-Chin, P. Chuan-Hsian, and L. Hoon-Jae. Indoor location tracking using received signal strength indicator. pages 229–256, 2011.

[6] C. David, C. Mario, and S. David de la Torre. Performance evaluation of bluetooth low energy in indoor positioning systems. *Trans. Emerging Telecommunications Technologies*, 25:1–10, 2014.

[7] T. Dinesh, A. Robert, and L. Xinrong. Indoor propagation modeling at 2.4 ghz for ieee 802.11 networks. In *6th IASTED International Multi-Conference on Wireless and Optical Communications. Banff, Canada*, 2006.

[8] A. Abdulrahman et al. Ultra wideband indoor positioning technologies: Analysis and recent advances. *Sensors (Basel)*, 16, 2016.

[9] A. Mandal et al. Beep: 3d indoor positioning using audible sound. In *Second IEEE Consumer Communications and Networking Conference, 2005*, pages 348–353, 2005.

[10] H. Andy et al. The anatomy of a context-aware application. 8:187–197, 2002.

[11] H.Liu et al. Survey of wireless indoor positioning techniques and systems. *IEEE TRANSACTIONS ON SYSTEMS, MAN, AND CYBERNETICS*, 37:1067–1080, 2007.

[12] J. Zhu et al. Rssi based bluetooth low energy indoor positioning. In *2014 International Conference on Indoor Positioning and Indoor Navigation (IPIN)*, pages 526–533, 2014.

[13] S. Gonzalo et al. Challenges in indoor global navigation satellite systems: Unveiling its core features in signal processing. *IEEE Signal Processing Society*, 29:230–250, 2012.

[14] W. Roy et al. The active badge location system. *ACM Transactions on Information Systems (TOIS)*, 10:91–102, 1992.

[15] Z. C. Jean et al. A 10-gram microflyer for vision-based indoor navigation. In *2006 IEEE/RSJ International Conference on Intelligent Robots and Systems*, pages 3267–3272, 2006.

[16] L. Hui, D. Houshang, B. Pat, and L. Jing. Survey of wireless indoor positioning techniques and systems. *IEEE Transactions on Systems, Man, and Cybernetics*, 37:1067–1078, 2007.

[17] Ville Kolehmainenn. Easyshopping - revolutionary personalized shopping experience, 2013.

[18] E. Mike and D. K. Mieso. Ieee 802.11 wlan based real-time location tracking in indoor and outdoor environments. In *2007 Canadian Conference on Electrical and Computer Engineering*, 2007.

[19] M. K. Mohamed, P. Sourav, and L. Alexander. Designing simple indoor navigation system for uavs. In *2011 19th Mediterranean Conference on Control and Automation (MED)*, pages 1223–1228, 2011.

[20] Navigation National Coordination Office for Space-Based Positioning and Timing. Gps accuracy, August 2017.

[21] C. Panarat and S. D. Joko. Indoor localization system using wireless sensor networks for stationary and moving target. In *2011 8th International Conference on Information, Communications and Signal Processing*, 2011.

[22] M. Rainer. *Indoor positioning technologies*. PhD thesis, Institute of Geodesy and Photogrammetry, Department of Civil, Environmental and Geomatic Engineering, ETH Zurich, 2012.

[23] F. Ramsey and H. Robert. Location fingerprinting with bluetooth low energy beacons. *IEEE Journal on Selected Areas in Communications*, 33, 2015.

[24] W. Roy. An introduction to rfid technology. *IEEE Pervasive Computing*, 5:25–33, 2006.

[25] H. Suining and S.-H. C. Gary. Wi-fi fingerprint-based indoor positioning: Recent advances and comparisons. *IEEE Communications Surveys and Tutorials*, 18:466–490, 2015.

[26] Cisco Systems. *Wi-Fi Location-Based Services 4.1 Design Guide*. Cisco Systems, 2008.

[27] D. Waltenegus and P. Christian. *Fundamentals of Wireless Sensor Networks*. Wiley, 1 2011.

[28] Wikipedia. Bluetooth low energy, 2018.

[29] G. Yanying and L. Anthony. A survey of indoor positioning systems for wireless personal networks. *IEEE Communications Surveys and Tutorials*, 11:13–32, 2009.

[30] F. Zahid, N. Rosdiadee, and I. Mahamod. Recent advances in wireless indoor localization techniques and system. *Computer Networks and Communications*, 2013, 2013.

# Appendices

# Appendix A

# Trilateration Results

## A.1 Results of Position (1,3)

Table A.1: Trilateration result of position 1,3.

| | Moving Average | Channel 1 | Channel 2 | Channel 3 |
|---|---|---|---|---|
| Actual 1 | 1.27,2.16 | 1.03,2.28 | 1.97,3.95 | 1.59,2.54 |
| Actual 2 | 1.20,1.97 | 2.07,3.13 | 0.18,2.10 | 1.11,2.68 |
| Actual 3 | 1.18,1.85 | 0.50,1.43 | 0.07,2.00 | 1.10,1.96 |
| Actual 4 | 2.20,2.78 | 1.06,1.97 | 2.00,2.02 | 1.59,2.63 |
| Actual 5 | 1.28,1.89 | 0.99,1.90 | 2.00,2.03 | 1.57,2.70 |

Table A.2: Absolute error of trilateration result of position 1,3.

| | Moving Average | Channel 1 | Channel 2 | Channel 3 |
|---|---|---|---|---|
| Actual 1 | 0.88 | 0.72 | 1.36 | 0.75 |
| Actual 2 | 1.05 | 1.08 | 1.22 | 0.34 |
| Actual 3 | 1.16 | 1.65 | 1.37 | 1.04 |
| Actual 4 | 1.22 | 1.03 | 1.40 | 0.70 |
| Actual 5 | 1.14 | 1.10 | 1.39 | 0.64 |

## A.2 Results of Position (1,1)

Table A.3: Trilateration result of position 1,1.

| | Moving Average | Channel 1 | Channel 2 | Channel 3 |
|---|---|---|---|---|
| Actual 1 | 1.66,1.19 | 1.68,0.91 | 1.94,1.14 | 1.78,1.38 |
| Actual 2 | 1.71,1.19 | 1.68,0.73 | 1.89,-0.49 | 1.81,0.63 |
| Actual 3 | 1.64,0.77 | 1.66,0.53 | 3.11,0.75 | 1.83,0.80 |
| Actual 4 | 1.59,1.10 | 1.63,1.11 | 1.95,-0.38 | 1.82,0.71 |
| Actual 5 | 1.69,1.45 | 1.60,1.19 | 3.07,0.61 | 1.83,0.92 |

Table A.4: Absolute error of trilateration result of position 1,1.

| | Moving Average | Channel 1 | Channel 2 | Channel 3 |
|---|---|---|---|---|
| Actual 1 | 0.69 | 0.69 | 0.95 | 0.87 |
| Actual 2 | 0.73 | 0.73 | 1.56 | 0.89 |
| Actual 3 | 0.68 | 0.81 | 2.12 | 0.85 |
| Actual 4 | 0.60 | 0.64 | 1.55 | 0.87 |
| Actual 5 | 0.82 | 0.63 | 2.07 | 0.83 |

## A.3 Results of Position (2,1)

Table A.5: Trilateration result of position 2,1.

| | Moving Average | Channel 1 | Channel 2 | Channel 3 |
|---|---|---|---|---|
| Actual 1 | 2.12,1.71 | 2.07,1.62 | 2.89,2.04 | 2.14,1.70 |
| Actual 2 | 2.00,1.48 | 1.91,1.54 | 1.85,1.99 | 2.07,1.70 |
| Actual 3 | 2.09,1.95 | 2.09,1.87 | 2.14,1.96 | 2.14,1.97 |
| Actual 4 | 1.99,1.57 | 1.92,1.26 | 1.92,1.60 | 2.04,1.70 |
| Actual 5 | 2.04,1.63 | 2.07,1.29 | 3.01,1.61 | 2.12,1.72 |

Table A.6: Absolute error of trilateration result of position 2,1.

| | Moving Average | Channel 1 | Channel 2 | Channel 3 |
|---|---|---|---|---|
| Actual 1 | 0.72 | 0.62 | 1.37 | 0.71 |
| Actual 2 | 0.48 | 0.55 | 1.00 | 0.70 |
| Actual 3 | 0.95 | 0.87 | 0.97 | 0.98 |
| Actual 4 | 0.57 | 0.27 | 0.61 | 0.70 |
| Actual 5 | 0.63 | 0.30 | 1.18 | 0.73 |

## A.4 Results of Position (3,3)

Table A.7: Trilateration result of position 3,3.

| | Moving Average | Channel 1 | Channel 2 | Channel 3 |
|---|---|---|---|---|
| Actual 1 | 2.35,2.74 | 2.09,2.73 | 2.01,2.24 | 2.19,2.36 |
| Actual 2 | 2.61,2.24 | 2.48,2.36 | 3.06,1.15 | 2.30,2.23 |
| Actual 3 | 2.33,2.37 | 2.09,2.76 | 2.04,2.23 | 2.21,2.37 |
| Actual 4 | 2.29,2.63 | 2.09,2.76 | 2.03,2.26 | 2.22,2.34 |
| Actual 5 | 2.29,2.52 | 2.09,2.79 | 2.00,2.29 | 2.21,2.34 |

Table A.8: Absolute error of trilateration result of position 3,3.

| | Moving Average | Channel 1 | Channel 2 | Channel 3 |
|---|---|---|---|---|
| Actual 1 | 0.70 | 0.95 | 1.25 | 1.03 |
| Actual 2 | 0.85 | 0.82 | 1.85 | 1.04 |
| Actual 3 | 0.92 | 0.94 | 1.23 | 1.01 |
| Actual 4 | 0.80 | 0.94 | 1.22 | 1.02 |
| Actual 5 | 0.86 | 0.93 | 1.23 | 1.03 |

## A.5 Results of Position (2,2)

Table A.9: Trilateration result of position 2,2.

| | Moving Average | Channel 1 | Channel 2 | Channel 3 |
|---|---|---|---|---|
| Actual 1 | 1.81,2.13 | 2.28,2.28 | 1.88,2.10 | 1.97,2.19 |
| Actual 2 | 2.21,2.04 | 2.52,2.11 | 2.72,1.30 | 1.96,2.19 |
| Actual 3 | 1.94,2.09 | 2.43,2.18 | 2.27,1.70 | 1.94,2.17 |
| Actual 4 | 1.89,1.89 | 2.43,2.22 | 1.78,2.17 | 1.97,2.04 |
| Actual 5 | 1.97,2.12 | 2.37,2.26 | 1.89,2.27 | 1.98,2.09 |

Table A.10: Absolute error of trilateration result of position 2,2.

| | Moving Average | Channel 1 | Channel 2 | Channel 3 |
|---|---|---|---|---|
| Actual 1 | 0.23 | 0.40 | 0.16 | 0.19 |
| Actual 2 | 0.21 | 0.53 | 1.00 | 0.19 |
| Actual 3 | 0.11 | 0.47 | 0.40 | 0.18 |
| Actual 4 | 0.16 | 0.48 | 0.28 | 0.05 |
| Actual 5 | 0.12 | 0.45 | 0.29 | 0.09 |